



Bachelor's thesis

# Dimuon production in deep inelastic scattering

**Submitted by**

Katrin Greve

**August 15, 2022**

First examiner
Priv.-Doz. Dr. Karol Kovarik

Second examiner
Prof. Dr. Michael Klasen

**Westfälische Wilhelms-Universität Münster**
**Fachbereich Physik**
**Institut für Theoretische Physik**

# Contents

# 1 Introduction

The aim of this thesis will be to discuss the proton structure and in particular the strange quark content of the proton. The strange content is relevant for measuring the Boson mass or other electroweak parameters that are not known yet, so in general it is the key to analyse data of current and future colliders. If one wants to explore and understand the proton further, there is no way around investigating and quantising the strange quark distribution. The first part of this thesis shows how the idea that the proton consists of individual partons has grown, starting with the idea of a point-like particle and ending with the parton model description. Therefor the elastic and deep inelastic electron proton scattering will be studied. The parton model describes each parton as a pointlike particle with its own parton distribution function (PDF) $q(x)$, where $x$ is the Bjorken scaling variable. As will be seen, the study of the proton with electromagnetic interactions is not sufficient to be sensitive for general linear combinations of strange and antistrange distribution functions $s(x)$ and $\overline{s}(x)$ so therefore it is necessary to do an examination of the proton in processes of weak interactions. The data of the Dimuon production cross section provides independent information on strange and antistrange quark distribution. But what exactly is the current state of research of strange content? Figure 1 shows the distribution functions for (anti)up, (anti)down, and (anti)strange quarks from PDF sets of different years. The CT sets are from the years 2006, 2014 and 2018 and the data of NNPDF3 is from 2021. We can see that the strange quark PDF and their uncertainty varies between the different data sets. The data sets from CT14 are from lepton deep-inelastic scattering experiments, and measurements of Drell-Yan processes and inclusive jet production [2]. A further development of the sets created from this are the CT18 PDF sets. These PDFs are produced by next-to-leading-order and next-to-next-to-leading-order perturbative QCD. The analysis included variety of new LHC data on production of single-inclusive jets, W/Z bosons and top-antitop quark pairs, obtained by the ATLAS, CMS and LHCb collaborations [5]. The data from NNPDF3 is accurate to next-to-next-to leading order pertubative Quantumchromodynamics (QCD) and includes charm-quark mass corrections to neutrino-nucleus structure functions. Especially there were used data from the NuTeV experiment, from several Tevatron and LHC experiments and from the NOMAD experiment. In the letter experiment they measure the ratio $R_{\mu\mu}$ of dimuon $\sigma_{\mu\mu}$ to inclusive charged-current cross sections $\sigma_{CC}$ [3]

$$R_{\mu\mu} = \frac{\sigma_{\mu\mu}}{\sigma_{CC}}. \tag{1}$$

Other interesting quantities to describe the strange fraction of the proton are the strange fraction of proton quark sea $R_s$ and the corresponding ratio of momentum fraction $\kappa$ [3], which are dependent on the Bjorken $x$. They are defined as

$$R_s = \frac{s(x) + \bar{s}(x)}{\bar{u}(x) + \bar{d}(x)} \quad \text{and} \quad \kappa = \frac{\int_0^1 x(s(x) + \bar{s}(x))}{\int_0^1 x(\bar{u}(x) + \bar{d}(x))}. \tag{2}$$

Figure 2 shows the ratio $R_s(x)$ at $Q = 1.6$ GeV for the four different data sets. In

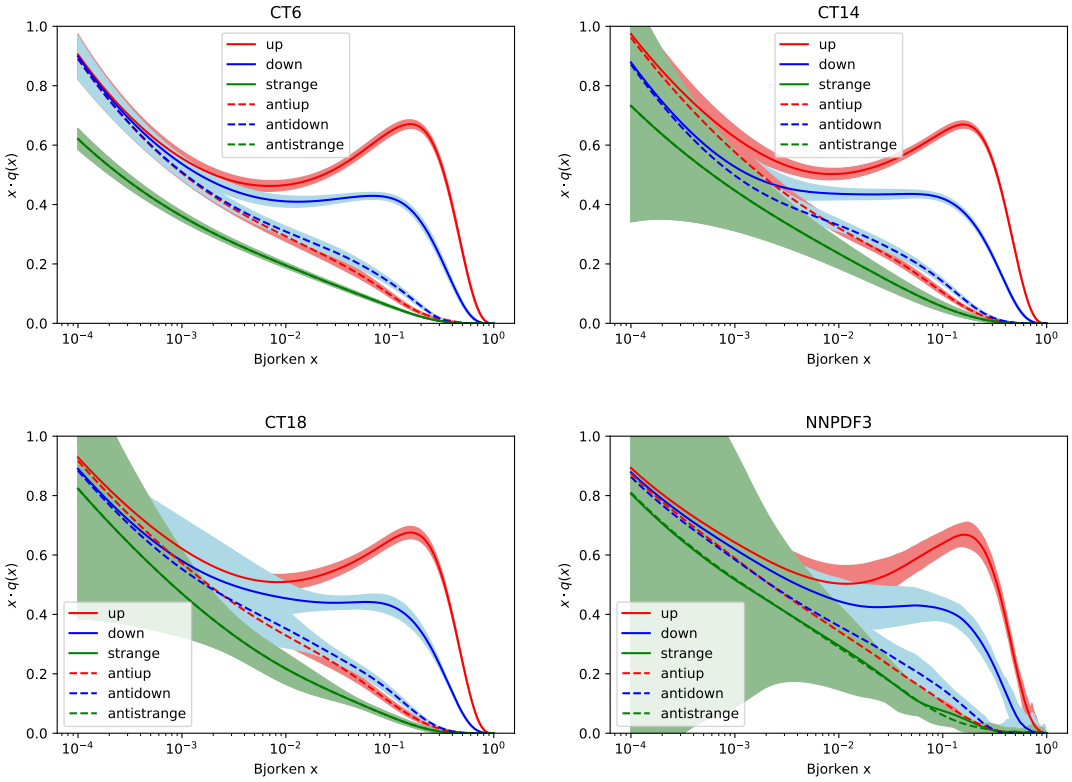


Figure 1: quark and antiquark distribution functions for the PDF sets CTEQ6, CT14, CT18 and NNPDF3.

current QCD there is the simplifying educated guess $s = \overline{s} = r \cdot \frac{\overline{u}+\overline{d}}{2}$ for small $x$ [6]. The figure shows that the ratio is nearly constant for all PDF data sets at small $x$ so the educated guess works, but the high uncertainties also show the lack of knowledge of the strange and antistrange distribution functions. Moreover the data sets from 2006 and 2014 predict a smaller strange ratio than the newer data sets from 2018 and 2021. In table 1 are the different values for $\kappa$ listed. It is noticeable that the data from NNPDF3 predict with $\kappa = 0.63$ a much higher ratio of momentum fraction than the CT data sets, especially a ratio >50%. It is also worth to mention that the NNPDF3 data predict

| PDF set | $\kappa$ | $\langle x \rangle_{s\_} = \int x(s - \overline{s})$ |
|---|---|---|
| CT6 | 0.39 | 0.0 |
| CT14 | 0.41 | 0.0 |
| CT18 | 0.37 | 0.0 |
| NNPDF3 | 0.63 | 0.001 |

Table 1: Momentum strange ratio and strange antisymmetry for different PDF sets.

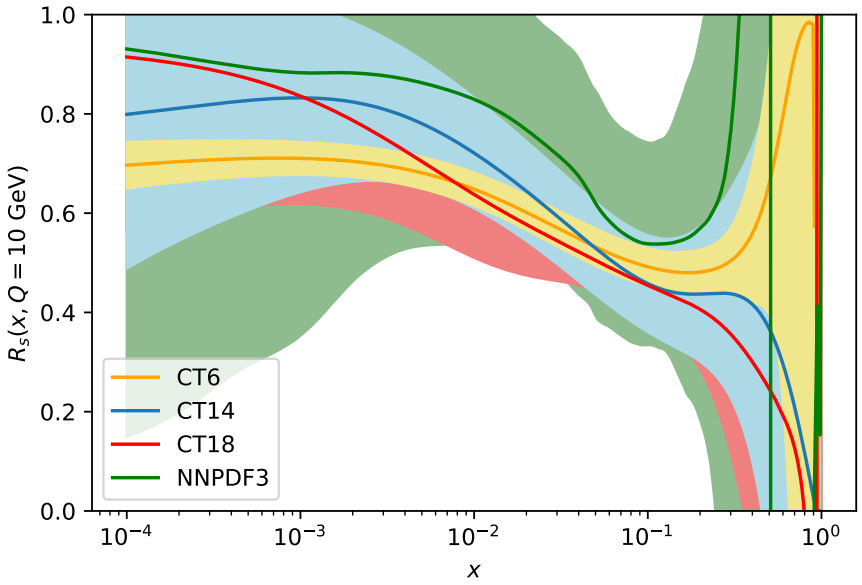


Figure 2: Strange ratio for different PDF sets.

an antisymmetry in strange and antistrange PDFs. The current knowledge is that the strangeness antisymmetry has a value of $-0.001 < \langle x \rangle_{s_-} < 0.005$ [3]. The fact that it is not even known if the antisymmetry is positive or negative is just another aspect of how much is still unexplored about the strange fraction of the proton.

## 2 In search of the structure of the proton

In order to investigate the structure of a particle, it is useful to measure the cross section in scattering experiments. The differential cross section is defined as the quotient of the particles counted in the solid angle per second and the number of incoming particles per second and area fraction. Expressed in a formula, in general the cross-section can be calculated by

$$d\sigma = \frac{\overline{|M|^2}}{F} dQ. \tag{3}$$

Here, $\overline{|M|^2}$ is the invariant amplitude, that can be calculated for different scattering processes. $F$ is the initial flux and $dQ$ the Lorentz-invariant phase space factor.
The possible resolution of the structure of a particle in scattering experiments is limited by the De Broglie wavelength of the incoming particles. To "see" a structure, the De Broglie wavelength

$$\lambda = \frac{h}{p} \tag{4}$$

has to be in the order of magnitude of the structure constant.
In the following sections, various cross sections are calculated using the Feynman rules, the commutator relations of the Dirac gamma matrices and trace theorems. These calculation rules can be found in the Appendix.

## 2.1 The proton as a point like particle: elastic electron-muon scattering

If the De Broglie wavelength of the scattering electrons is larger than the spatial expansion of the proton, the electrons would "see" just a pointlike particle. The proton then has the same electron scattering behaviour as the muon, we just have to use the mass of the proton $M$ instead the mass of the muon $m_\mu$. In the following section the crossing section of elastic electron-muon scattering will be calculated in order to get a result for scattering with pointlike particles. We will see that this calculation can also be used for the scattering of quarks.
The Feynman diagram for this scattering process is shown in fig. 3. The electron carries

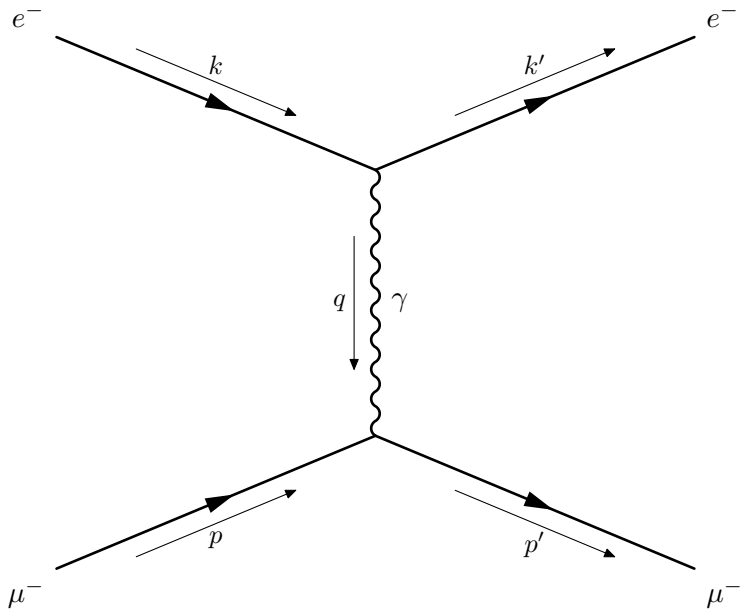


Figure 3: The leading order Feynman diagram for electron-muon scattering

the four-momentum $k$ before scattering and $k'$ after scattering. The four-momentum of the muon is $p$ before and $p'$ after. The calculation of the initial flux and the Lorentz invariant phase space factor is shown in eq. (A.16) and eq. (A.19). The invariant amplitude consists of the two particle currents (they build up a scalar separately) and the photon propagator, that can be written in the form $\left(-\frac{ig_{\mu\nu}}{q}\right)$. Here, $q$ is the four-momentum, that is transmitted at the scattering process. As we can see in the Feynman diagram,

this scattering is a $t$-channel process, so $q^2 = t = (k - k')^2$ is the transmitted four-momentum (see eq. (A.5)). Now $M$ and $M^\dagger$ can be calculated by using the Feynman rules from

$$\begin{aligned} M &= [\bar{u}^{s_1}(k')ie\gamma^\mu u^{s_2}(k)][\bar{u}^{s_3}(p')ie\gamma^\nu u^{s_4}(p)]\left(-\frac{ig_{\mu\nu}}{t}\right) \\ &= i\frac{e^2}{t}[\bar{u}^{s_1}(k')\gamma^\mu u^{s_2}(k)][\bar{u}^{s_3}(p')e\gamma_\mu u^{s_4}(p)] \end{aligned}$$

$$\begin{aligned} M^\dagger &= -i\frac{e^2}{t}[u^{s_2\dagger}(k)\gamma^{\alpha\dagger}\bar{u}^{s_1\dagger}(k')][u^{s_4\dagger}(p)(\gamma_\alpha)^\dagger\bar{u}^{s_3\dagger}(p')] \\ &= -i\frac{e^2}{t}[\bar{u}^{s_2}(k)\gamma^\alpha u^{s_1}(k')][\bar{u}^{s_4}(p)\gamma_\alpha u^{s_3}(p')] \end{aligned}$$

The invariant amplitude can be written in the form

$$\overline{|M|^2} = \frac{e^4}{t^2}L_e^{\mu\alpha}L_{\mu\alpha}^{\text{muon}} \tag{5}$$

because the Electron current $L_e^{\mu\alpha}$ as well as the muon current form a Lepton tensor, that can be calculated independently. It has to be considered that there is no knowledge about the spin states of the particles. This is why we have to average over all spins by summing over all spin states and dividing by two. So the $e^-$ current is:

$$\begin{aligned} L_e^{\mu\alpha} =& \frac{1}{2}\sum_{s_1,s_2}[\bar{u}^{s_1}(k')ie\gamma^\mu u^{s_2}(k)][\bar{u}^{s_2}(k)\gamma^\alpha u^{s_1}(k')] \\ &= \frac{1}{2}\text{Tr}[(\not{k}' + m_e)\gamma^\mu(\not{k} + m_e)\gamma^\alpha] \\ &= \frac{1}{2}\text{Tr}(\not{k}'\gamma^\mu\ \not{k}\gamma^\alpha) + \frac{1}{2}m_e^2\text{Tr}(\gamma^\mu\gamma^\alpha) \\ &= 2k'_\rho k_\sigma(g^{\rho\mu}g^{\sigma\alpha} - g^{\rho\sigma}g^{\mu\alpha} + g^{\rho\alpha}g^{\sigma\mu}) + 2m_e^2 g^{\mu\alpha} \\ &= 2(k'^\mu k^\alpha + k'^\alpha k^\mu + g^{\mu\alpha}(m_e^2 - (k'\cdot k))) \end{aligned} \tag{6}$$

We achieve the following reslut for the muon current performing the equivalent calculation:

$$L_{\mu\alpha}^{\text{muon}} = 2(p'_\mu p_\alpha + p'_\alpha p_\mu + g_{\mu\alpha}(m_\mu^2 - (p'\cdot p)))$$

Now $\overline{|M|^2}$ can be calculated by expanding all products:

$$\begin{aligned} \overline{|M|^2} &= \frac{e^4}{t^2}2(k'^\mu k^\alpha + k'^\alpha k^\mu + g^{\mu\alpha}(m_e^2 - (k'\cdot k)))2(p'_\mu p_\alpha + p'_\alpha p_\mu + g_{\mu\alpha}(m_\mu^2 - (p'\cdot p))) \\ &= 4\frac{e^4}{t^2}[(2(k'\cdot p)(k\cdot p') + 2(k'\cdot p')(k\cdot p) + 2(m_e^2 - (k'\cdot k))(p'\cdot p) + 2(m_\mu^2 - (p'\cdot p))(k'\cdot k) \\ &+ 4m_e^2 m_\mu^2 + 4(p'\cdot p)(k'\cdot k) - 4m_e^2(p'\cdot p) - 4M^2(k'\cdot k)] \\ &= 8\frac{e^4}{t^2}[(k'\cdot p)(k\cdot p') + (k'\cdot p')(k\cdot p) - m_e^2(p'\cdot p) - m_\mu^2(k'\cdot k) + 2m_e^2 m_\mu^2] \end{aligned} \tag{7}$$

In the extreme relativistic limit we can neglect the electron mass as well as the muon mass ($m_e \approx m_\mu \approx 0$). Moreover we can use the invariant Mandelstam variables eq. (A.5), so the expression in eq. (7) can be written in the form:

$$\begin{aligned}\overline{|M|^2} &= 8\frac{e^4}{t^2}[\underbrace{(k'\cdot p)}_{u/2}\underbrace{(k\cdot p')}_{u/2} + \underbrace{(k'\cdot p')}_{s/2}\underbrace{(k\cdot p)}_{s/2}] \\ &= 2e^4\ \frac{s^2+u^2}{t^2} \end{aligned} \tag{8}$$

Comparing this calculation with the scattering process of the Proton, it also makes sense to calculate the cross section without neglecting the mass of the muon, because the proton is much heavier. Moreover it is useful to replace $p'$ by

$$p' = k + p - k'$$

to reduce the equation to the momenta before scattering and the electron momentum after scattering. With this replacement there is no need to measure the proton momentum after scattering. In the following only the electron mass will be neglected, $p'$ will be replaced and $q^2 \approx -2(k\cdot k')$ in eq. (7) will be used, so the equation becomes

$$\overline{|M|^2} = 8\frac{e^4}{t^2}[-\frac{1}{2}q^2((k\cdot p)-(k'\cdot p)) + 2(k\cdot p)(k'\cdot p) + \frac{1}{2}m_\mu^2 q^2].$$

To simplify the equation it is useful to look at the process from the laboratory frame, in which the muon is in rest $p = (m_\mu, 0)$. The energy of the electron before scattering is $E$, after scattering $E'$. The equation simplifies to:

$$\overline{|M|^2} = 16\frac{e^4}{t^2}m_\mu^2 EE'\left(1 + \frac{\frac{1}{2}m_\mu^2 q^2}{2m_\mu^2 EE'} - \frac{\frac{1}{2}q^2 m_\mu^2 (E-E')}{2m_\mu^2 EE'}\right)$$

At this point we can take advantage of $q^2 = t$, because with eq. (A.7) for $t$ in the laboratory frame, we can exchange $q$ by an expression of $E'$ and $\theta$

$$\begin{aligned}\overline{|M|^2} &= 16\frac{e^4}{t^2}m_\mu EE'(1-\sin^2\theta - \frac{q^2}{2m_\mu^2}\sin^2\theta) \\ &= 16\frac{e^4}{t^2}m_\mu^2 EE'(\cos^2\theta - \frac{q^2}{2m_\mu^2}\sin^2\theta) \\ &= 256\frac{\alpha^2\pi^2}{q^4}m_\mu^2 EE'(\cos^2\theta - \frac{q^2}{2m_\mu^2}\sin^2\theta)\end{aligned}$$

The elementary charge was replaced by the fine structure constant $\alpha = \frac{e^2}{4\pi}$. By using eq. (3), the initial flux and the Lorentz invariant phase space factor in the laboratory

frame A.19, the differential cross section becomes:

$$d\sigma_{\text{Lab}} = \underbrace{\frac{1}{4m_\mu E}}_{F} \underbrace{256\frac{\alpha^2\pi^2}{q^4}m_\mu^2 EE'(\cos^2\theta - \frac{q^2}{2m_\mu^2}\sin^2\theta)}_{\overline{|M|^2}} \underbrace{E'dE_{k'}d\Omega\frac{1}{16\pi^2 m_\mu A}\delta(E' - \frac{E}{A})}_{dQ_{Lab}}$$
$$= 4\frac{\alpha^2}{q^4}E'^2(\cos^2\theta - \frac{q^2}{2m_\mu^2}\sin^2\theta)\frac{1}{A}\delta(E' - \frac{E}{A})dE'd\Omega$$

Now we can perform the integration over $E'$. After that we substitute $A = \frac{E}{E'}$ and $q^4 = t^2 = 16E^2E'^2\sin^4\frac{\theta}{2}$, see eq. (A.7).

$$\left(\frac{d\sigma}{d\Omega}\right)_{\text{Lab}} = \left(\frac{\alpha}{2E\sin^2\frac{\theta}{2}}\right)^2 \frac{E'}{E}(\cos^2\theta - \frac{q^2}{2m_\mu^2}\sin^2\theta) \tag{9}$$

Again, written in terms of the scattering angle $\theta$ (see eq. (A.18) instead of eq. (A.19)) we get

$$\frac{d\sigma}{dE'd\Omega} = 4\frac{\alpha^2}{q^4}E'^2(\cos^2\theta - \frac{q^2}{2m_\mu^2}\sin^2\theta)\delta(v - \frac{q^2}{2m_\mu}) \tag{10}$$

which is the final result for the electron muon differential cross section. This result is essential, because all cross sections of scattering processes of point like spin $\frac{1}{2}$ particles can be written in this form. In the following sections we show, that the cross section of the proton is not equal to the electron-muon cross section with exchanged masses. Nonetheless, the calculation above can be used for comparison and especially to determine the deviations that arise from the parton model.

## 2.2 Spatially extended Proton: elastic electron-proton scattering

If the electrons have a higher kinetic energy, their De Broglie wavelength would be in the order of the spatial expansion of the proton. The electrons now "see" the proton as an expanded particle. The elastic electron proton scattering process is show in fig. 4. One can see that the proton is mentioned with an expansion, but the electrons are not fast enough to notice a possible inner structure. The proton current can in general be written as

$$J_P^\mu = e\bar{u}(p')[...]u(p)e^{i(p'-p)x}.$$

The brackets [...] can not simply be replaced by $\gamma^\mu$ as for the muon scattering, because the Proton does not act like a point like Spin-$\frac{1}{2}$-particle. Instead we exchange [...] by a general expression:

$$[...] = \left[F_1(q^2)\gamma^\mu + \frac{\kappa}{2M}F_2(q^2)i\sigma^{\mu\nu}q_\nu\right] \tag{11}$$

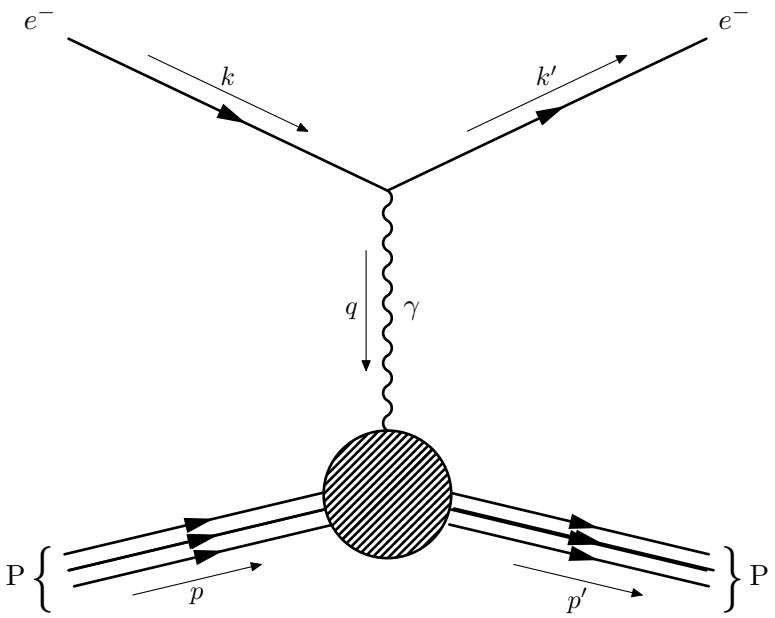


Figure 4: The leading-order Feynman diagram for elastic Electron proton scattering.

Here $\kappa$ is the anomalous magnetic moment and $F_1$, $F_2$ present two independent form factors. The boundary conditions $q^2 \to 0$ are known, because for small transmitted four-momenta we see just a particle with charge $e$ and magnetic moment $(1+\kappa)\frac{e}{2M}$, so $F_1(0) = F_2(0) = 1$. We can calculate the cross section equivalent to the cross section of electron-muon scattering but with the new expression for the proton current. We can write:

$$\left(\frac{d\sigma}{d\Omega}\right)_{\text{Lab}} = \left(\frac{\alpha}{2E\sin^2\frac{\theta}{2}}\right)^2 \frac{E'}{E}\left((F_1^2 - \frac{\kappa^2 q^2}{4M^2}F_2^2)\cos^2\theta - (F_1+\kappa F_2)^2\frac{q^2}{2M^2}\sin^2\theta\right) \quad (12)$$

This formula is known as the Rosenbluth-formula. We can avoid intereference terms by using $G_E = F_1 + \frac{\kappa q^2}{4M^2}F_2$ und $G_M = F_1\kappa F_2$. If we also use $\tau = -\frac{q^2}{4M^2}$, then the Rosenbluth-formula is

$$\left(\frac{d\sigma}{d\Omega}\right)_{\text{Lab}} = \left(\frac{\alpha}{2E\sin^2\frac{\theta}{2}}\right)^2 \frac{E'}{E}\left(\frac{G_E^2 + \tau G_M^2}{1+\tau}\cos^2\theta + 2\tau G_M^2\sin^2\theta\right). \quad (13)$$

Now, interference terms do not appear. In equivalence to eq. (10) the formula can be written as:

$$\frac{d\sigma}{dE'd\Omega} = 4\frac{\alpha^2}{q^4}E'^2\left(\frac{G_E^2 + \tau G_M^2}{1+\tau}\cos^2\theta + 2\tau G_M^2\sin^2\theta\right)\delta(v + \frac{q^2}{2M}) \quad (14)$$

The cross section is the result for the interaction in which the proton is described as a particle with expansion but without an inner structure. If one measures this cross section

experimentally with a higher kinetic energy for the electrons, there are two possibilities: Either the proton has no internal structure and the electron-proton scattering is completely described, or the proton has an inner structure and the electrons with which the scattering was performed have enough energy to break up the proton, so that inelastic scattering can be observed. This possibility is described in the following section.

### 2.3 The proton with inner structure: inelastic electron-proton scattering

The calculation for the cross section of the inelastic electron-proton scattering is also based on the calculation for the electron-muon scattering. The Feynman diagram for inelastic electron proton scattering is shown in fig. 5. However, here is $d\sigma \sim L^e_{\mu\nu} W^{\mu\nu}$,

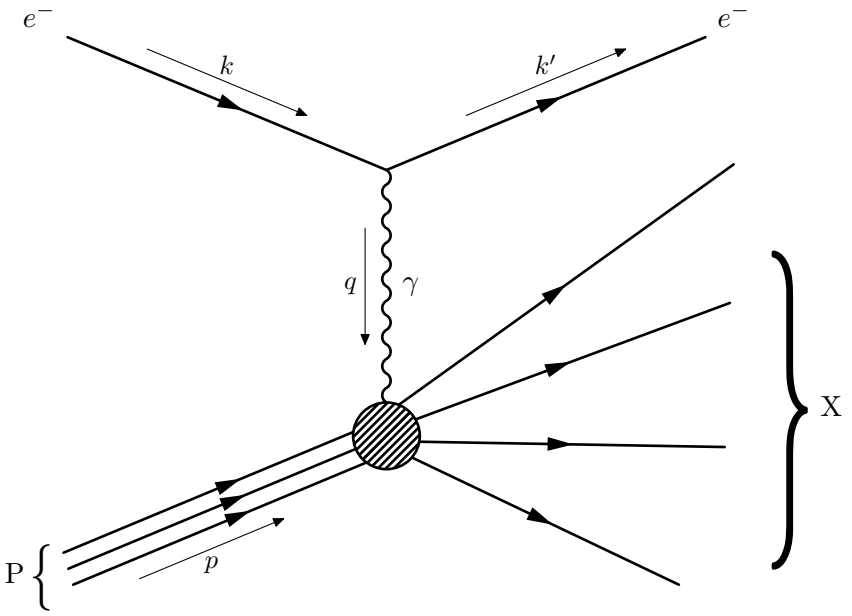


Figure 5: The lowest order Feynman diagramm for inelastic Electron proton scattering.

where $W^{\mu\nu}$ describes the expression for the hadronic tensor, which is first presented in its most general form. For now, the only certainty is that it must be symmetrical in $\mu \leftrightarrow \nu$, because $L^e_{\mu\nu}$ from eq. (6) is symmetrical and all antisymmetrical terms are omitted after summation via Einstein's summation convention. Furthermore, $W^{\mu\nu}$ is a function of $g^{\mu\nu}$, $p$ and $q$. $\gamma^\mu$ is not included because the cross section is treated here, where the spins have already been summed and averaged. The tensor is therefore in the form

$$W^{\mu\nu} = -W_1 g^{\mu\nu} + \frac{W_2}{M^2} p^\mu p^\nu + \frac{W_4}{M^2} q^\mu q^\nu + \frac{W_5}{M^2}(p^\mu q^\nu + p^\nu q^\mu). \tag{15}$$

$W_3$ is reserved for an antisymmetric component. We will see that antisymmetry contributes to the calculation in neutrino scattering. By a generalised form of the continuity equation, $q_\mu W^{\mu\nu} = 0$ must hold which is known as the Ward identity [4]. From this follows:

$$\begin{aligned} q_\mu W^{\mu\nu} &= -W_1 q_\mu g^{\mu\nu} + \frac{W_2}{M^2} q_\mu p^\mu p^\nu + \frac{W_4}{M^2} q_\mu q^\mu q^\nu + \frac{W_5}{M^2}(q_\mu p^\mu q^\nu + q_\mu p^\nu q^\mu) \\ &= -W_1 q^\nu + \frac{W_2}{M^2}(q\cdot p)p^\nu + \frac{W_4}{M^2} q^2 q^\nu + \frac{W_5}{M^2}((q\cdot p)q^\nu + p^\nu q^2) \\ &= q^\nu \underbrace{(-W_1 + \frac{w_2}{M^2}q^2 + \frac{w_5}{M^2}(q\cdot p))}_{=0} + p^\nu \underbrace{(\frac{w_2}{M^2}(q\cdot p) + \frac{w_5}{M^2}q^2)}_{=0} \stackrel{!}{=} 0 \end{aligned}$$

For this equation to yield 0 in general, the coefficients in front of $q^\nu$ and $p^\nu$ must cancel separately. We see, this causes the dependence relations:

$$\begin{aligned} W_5 &= -\frac{q\cdot p}{q^2} W_2, \\ W_4 &= \frac{M^2}{q^2} W_1 - \frac{q\cdot p}{q^2} W_5 = \frac{M^2}{q^2} W_1 + \frac{(q\cdot p)^2}{q^4} W_2. \end{aligned}$$

Thus only two of the four assumed structure functions are independent of each other and we can write $W^{\mu\nu}$ as

$$W^{\mu\nu} = W_1(-g^{\mu\nu} + \frac{q^\mu q^\nu}{q^2}) + \frac{W_2}{M^2}(p^\mu - \frac{q\cdot p}{q^2}q^\mu)(p^\nu - \frac{q\cdot p}{q^2}q^\nu). \tag{16}$$

At this point it should be noted that the tensor is dependent on two independent variables. Here one often uses $q^2$ and $v = \frac{p\cdot q}{M}$. Later one sees that also the choice of

$$x = -\frac{q^2}{2p\cdot q} = -\frac{q^2}{2Mv} \tag{17}$$

$$y = \frac{p\cdot q}{p\cdot k} = 1 - \frac{E'}{E} \tag{18}$$

can be useful as independent variables. To calculate the cross section of the electron-proton scattering, the product $L^e_{\mu\nu} W^{\mu\nu}$ is evaluated. For this purpose, the result from eq. (6) from the electron-muon scattering is used for $L^e_{\mu\nu}$:

$$\begin{aligned} & L^e_{\mu\nu} W^{\mu\nu} \qquad (19) \\ =& 2[k'_\mu k^\nu + k'_\nu k_\mu + g_{\mu\nu}(m_e^2 - (k'\cdot k))][W_1(-g^{\mu\nu} + \cancel{\frac{q^\mu q^\nu}{q^2}}) + \frac{W_2}{M^2}(p^\mu - \frac{q\cdot p}{q^2}\cancel{q^\mu})(p^\nu - \frac{q\cdot p}{q^2}\cancel{q^\nu})] \end{aligned}$$

The terms that are crossed out fall directly due to

$$\begin{aligned} q_\mu L_e^{\mu\nu} &= 2(k_\mu - k'_\mu)[k'^\mu k^\alpha + k'^\alpha k^\mu + g^{\mu\alpha}(m_e^2 - (k'\cdot k))] \\ &= 2[k^\nu(k'\cdot k) - k^\nu m_e^2 + k'^\nu m_e^2 - k'^\nu(k'\cdot k) \\ &\quad + k^\nu m_e^2 - k^\nu(k'\cdot k) - k'^\nu m_e^2 + k'^\nu(k'\cdot k)] \\ &= 0 \end{aligned} \tag{20}$$

With this we can simplify eq. (19) to

$$
\begin{aligned}
&L^e_{\mu\nu}W^{\mu\nu} \\
&= -2W_1(k\cdot k') - 2W_1(k\cdot k') + 8W_1(k\cdot k') + \frac{2W_2}{M^2}(2(k'\cdot p)(k\cdot p) + \underbrace{m_e^2}_{\approx 0}\, p^2 - \underbrace{p^2}_{M^2}(k\cdot k')) \\
&= 4W_1(k\cdot k') + 2\frac{W_2}{M^2}(2(k'\cdot p)(k\cdot p) - M^2(k\cdot k')). \qquad (21)
\end{aligned}
$$

If one considers the scattering in the laboratory system, i.e. in the rest system of the proton, the scalar products can be expressed with the help of the relations from eq. (A.7) via $E'$ and $\theta$. It follows

$$
L^e_{\mu\nu}W^{\mu\nu} = 4EE'(2W_1 \sin^2\frac{\theta}{2} + W_2\cos^2\frac{\theta}{2}). \qquad (22)
$$

The invariant amplitude is then equivalent to eq. (5) with an additional normalisation $4\pi M$ to

$$
\begin{aligned}
\overline{|M|^2} &= 4\pi M\frac{e^4}{q^4}4EE'(2W_1\sin^2\frac{\theta}{2} + W_2\cos^2\frac{\theta}{2}) \\
&= \frac{16\cdot 16M\alpha^2\pi^3}{q^4}EE'(2W_1\sin^2\frac{\theta}{2} + W_2\cos^2\frac{\theta}{2}).
\end{aligned}
$$

Here, the fine structure constant $\alpha$ was used again. The total cross section corresponds to the term:

$$
d\sigma = \frac{1}{4ME}\frac{16\cdot 16M\alpha^2\pi^3}{q^4}EE'(2W_1\sin^2\frac{\theta}{2} + W_2\cos^2\frac{\theta}{2})\frac{d^3\vec{k}'}{2E'(2\pi)^3}
$$

It should be noted that the Lorentz-invariant phase space element here only runs over $\vec{k}'$ (see eq. (A.17)), since nothing is known about the final momentum $\vec{X}$. This information is contained in the structure factors $W_1$ and $W_2$. It follows

$$
\frac{d\sigma}{dE'd\Omega} = 4\frac{\alpha^2E'^2}{q^4}(2W_1\sin^2\frac{\theta}{2} + W_2\cos^2\frac{\theta}{2}). \qquad (23)
$$

This is the most general expression for the cross section of the inelastic electron-proton scattering. The structure functions keep open what the inner structure of the proton looks like.

## 2.4 Comparison

It is useful to make a short summary of the results so far, to use them for future references. In the laboratory frame and a neglected electron mass all three differential cross sections can be written in the form

$$
\frac{d\sigma}{dE'd\Omega} = \frac{4\alpha^2E'^2}{q^4}\{...\}
$$

with

$$\{...\} = (\cos^2\theta - \frac{q^2}{2m^2}\sin^2\theta)\delta(v + \frac{q^2}{2m})$$

for muons or other point like particles (by replacing mass and charge),

$$\{...\} = \left(\frac{G_E^2 + \tau G_M^2}{1+\tau}\cos^2\theta + 2\tau G_M^2 \sin^2\theta\right)\delta(v + \frac{q^2}{2M})$$

for an expanded particle and finally

$$\{...\} = (2W_1 \sin^2\frac{\theta}{2} + W_2\cos^2\frac{\theta}{2})$$

when the electron breaks up the proton target and reveals the inner structure in form of $W_1$ and $W_2$.
The actual expressions for $W_1$ and $W_2$ are discussed in the following chapter.

# 3 Partons and Bjorken scaling

At small wavelengths, the experimental results provide that the proton behaves like a free Dirac particle [4], which is reflected in

$$2mW_1 = \frac{Q^2}{2m}\delta(v - \frac{Q^2}{2m}) = 2mW_1(v, Q^2)$$
$$W_2 = \delta(v - \frac{Q^2}{2m}) = W_2(v, Q^2)$$

For convinience the positive variable $Q^2 = -q^2$ is used. With the calculation rules of the delta function one can see that

$$2mW_1 = \frac{Q^2}{2mv}\delta(1 - \frac{Q^2}{2mv}) = 2mW_1(\omega) \equiv 2F_1$$
$$vW_2 = \delta(1 - \frac{Q^2}{2mv}) = vW_2(\omega) \equiv F_2 \tag{24}$$

so that the structure functions $W_1$ and $W_2$ are in the form of a delta function and only depend on the variable $\omega = \frac{2mv}{Q^2}$. Thus, the virtual photon interacts with point-like particles. The proton consists of many point-like particles called partons, which we do not have to identify them yet as quarks and gluons. Each parton can carry a different fraction $x = \frac{1}{\omega}$ of the total momentum and energy of the proton, it has the momentum $\hat{p} = xp$. The variables with a roof each refer to a single parton. If we consider the scattering in the rest system of the proton, i.e. $p = (M, 0)$, it can easily be shown that $x$ and $y$ each lie between 0 and 1:
The so-called invariant mass, $W^2 = (p+q)^2 = M^2 + q^2 + 2Mv$ fulfils $W^2 > M^2$ so we get $-q^2 < 2Mv$. Furthermore, for $q^2$, neglecting the electron mass, $q^2 = -2EE'(1-\cos\Theta) <$

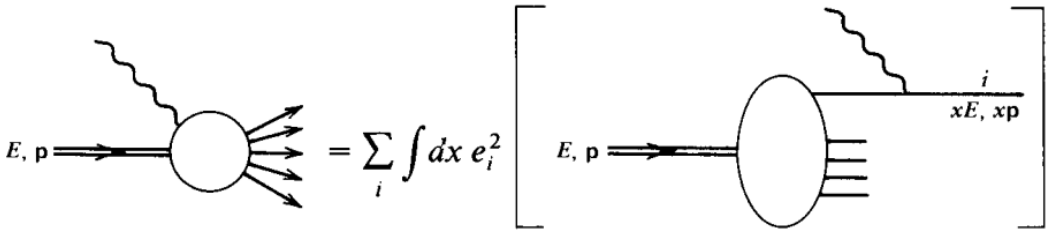


Figure 6: Illustration of the parton model, according to which the cross section of the electron-proton scattering can be expressed via the individual interactions with the partons. [4].

0 holds. Thus is $0 < x < 1$. For $y$ in the laboratory system $y = \frac{M(E-E')}{ME} = 1 - \frac{E'}{E}$ holds. Since $E' < E$ we directly get $0 < y < 1$.
As has been shown, the variable $x$ lies between 0 and 1, which fits the interpretation as a momentum fraction. At this point it makes sense to introduce the parton distribution functions (PDFs):

$$f_i(x) = \frac{dp_i}{dx}, \tag{25}$$

$$\sum_i \int dx f_i(x) = 1. \tag{26}$$

$f_i(x)$ describes the probability that parton $i$ carries the momentum part $x$ of the proton momentum. Since the entire proton momentum is distributed among the partons, the completeness relation from eq. (26) applies. The aim is now to express the effective cross section of the proton scattering via the individual effective cross sections of the partons in order to be able to draw conclusions about the intrinsic structure of the proton. This idea is visualised in fig. 6. In the form of an equation this connection can be written as

$$\left(\frac{d\sigma}{dtdu}\right)_{eP\to eX} = \sum_i \int dx f_i(x) \left(\frac{d\sigma}{dtdu}\right)_{eq_i\to eq_i}. \tag{27}$$

First we want to calculate the right side of the equation, $\left(\frac{d\sigma}{dtdu}\right)_{eq_i\to eq_i}$, the cross section for elastic electron parton scattering.

### 3.1 Elastic electron-quark scattering

The Feynman diagram of this parton scattering, which we now assume to be a quark scattering, is shown in fig. 7. The remaining partons of the proton are labeled as "Spectators ". To calculate this cross section, in the first step, the invariant Mandelstam variables of the single parton can be considered, for which holds:

$$\hat{s} = xs, \quad \hat{t} = t \ \text{ and } \ \hat{u} = xu. \tag{28}$$

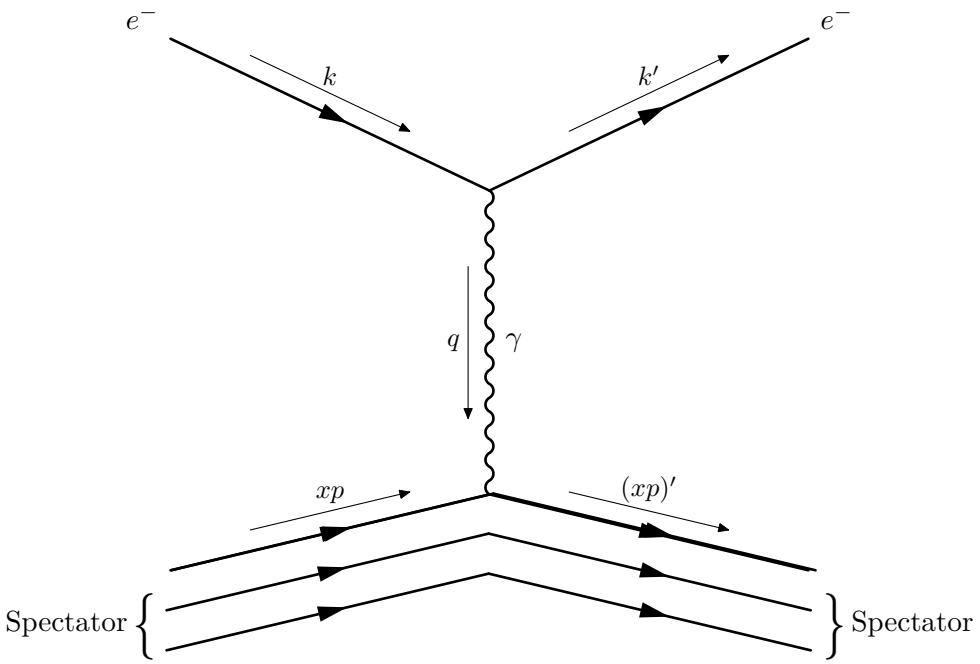


Figure 7: The lowest order Feynman diagram for elastic electron-quark scattering

Furthermore, we take advantage of the fact that

$$\cos\theta = \frac{-\frac{1}{2}s(1-\cos\theta)+\frac{1}{2}s(1+\cos\theta)}{s} = \frac{t-u}{s}$$

applies (see eq. (A.6)). Now $d\cos\theta$ can be expressed over $dt$ using the derivative $\frac{d\cos\theta}{dt} = \frac{1}{s}$. The effective cross-section that results from eq. (3), the result from eq. (8) from the electron-muon scattering calculation for the invariant amplitude and the Lorentz-invariant phase element in the CMS (eq. (A.20)) thus becomes:

$$\begin{aligned}\left(\frac{d\sigma}{d\Omega}\right)_{\text{muon}} &= \frac{1}{64\pi^2 s} 2e^4 \frac{s^2+u^2}{t^2} \\ \Rightarrow \left(\frac{d\sigma}{dt}\right)_{\text{Parton}} &= \frac{2\pi\alpha^2 e_i^2}{s^2}\frac{s^2+u^2}{t^2}\end{aligned}$$

Here, the integration over $\phi$ was carried out and $\alpha = \frac{e^2}{4\pi}$ was used. Furthermore, we have $\alpha \to \alpha e_i$ in electron-quark scattering where $e_i$ describes the charge fraction carried by the parton. We have used the invariant amplitude that neglect the muon mass, or in this case the quark mass, because if the electrons have enough kinetic energy to break up the proton we can be sure that we are in range of the extreme relativistic limit, where the masses can be neglected. Now, in addition, eq. (A.13) and eq. (28) can be used to

rewrite the effective cross-section in the form

$$\begin{aligned}\left(\frac{d\sigma}{dtdu}\right)_{eq_i\to eq_i} &= x\frac{d\sigma}{d\hat{t}d\hat{u}} \\ &= \frac{2\pi\alpha^2 e_i^2}{s^2}\frac{s^2+u^2}{t^2}\delta(u+\frac{t}{x}+s) \\ &= x2\pi\frac{\alpha^2 e_i^2}{t^2 s^2}\frac{s^2+u^2}{s+u}\delta(x+\frac{t}{(u+s)}).\end{aligned}$$

This is the result for the cross section for elastic electron-quark scattering and the right-hand side of eq. (27).

### 3.2 Master formula of the parton model

The left-hand side of the equation can be expressed using the result of eq. (8) (neglecting the term with prefactor $M^2$) and the relations of $s$, $t$, $u$ from eq. (A.5). It thus holds:

$$\begin{aligned}L^e_{\mu\nu}W^{\mu\nu} &= -2tW_1 - \frac{W_2}{M^2}su \\ &= -\frac{2t}{M}F_1 - \frac{su}{vM^2}F_2 \\ &= \frac{2}{M(s+u)}[(s+u)^2 xF_1 - usF_2].\end{aligned}$$

In the last step we use eq. (A.13) and $v = E - E' = \frac{s+u}{2M}$. Furthermore, the differential cross section according to $dtdu$ and not according to $d\Omega dE'$ is required. Considering in the laboratory frame $s = 2ME$, $t = q^2 = -2EE'(1-\cos\theta)$ and $u = -2ME'$ one obtains

$$\begin{aligned}d\Omega = d\cos\theta d\phi = -2\pi\frac{1}{2EE'}dt = 4\pi\frac{M^2}{su}dt \\ dE' = -\frac{1}{2M}du.\end{aligned}$$

This can be used in the differential cross section.

$$\begin{aligned}\frac{d\sigma}{dudt} &= \underbrace{\frac{1}{4ME}}_{1/F}\underbrace{4\pi M\frac{e^4}{q^4}\frac{2}{M(s+u)}[(s+u)^2xF_1 - usF_2]}_{|\bar{M}|^2}\underbrace{\frac{E'}{16\pi^3}d\Omega dE'}_{dQ} \\ &= \frac{1}{4ME}4\pi M\frac{e^4}{q^4}\frac{2}{M(s+u)}[(s+u)^2xF_1 - usF_2]\frac{E'}{16\pi^3}\frac{-1}{2M}4\pi\frac{M^2}{su}dtdu\end{aligned}$$

In the next step, with the same relations as just mentioned, $E = \frac{s}{2M}$, $E' = -\frac{u}{2M}$, $q^4 = t^2$ and $e^4 = 16\pi^2\alpha^2$ can be substituted.

$$\begin{aligned}\frac{d\sigma}{dudt} &= \frac{2M}{4Ms} 4 \cdot 16\pi^3 M \frac{\alpha^2}{t^2} \frac{2}{M(s+u)} [(s+u)^2 xF_1 - usF_2] \frac{-u}{2M16\pi^3} \frac{-1}{2M} 4\pi \frac{M^2}{su} dtdu \\ &= 4\pi \frac{\alpha^2}{s^2t^2} \frac{1}{(s+u)} [(s+u)^2 xF_1 - usF_2] \\ &= 4\pi \frac{\alpha^2}{s^2t^2} \frac{1}{(s+u)} [(s^2+u^2)xF_1 + us(x2F_1 - F_2)]\end{aligned}$$

This is the final expression for the left side of eq. (27). Both expressions can now be substituted into the equation and the integration over $x$ can be performed. This results in:

$$\begin{aligned}4\pi \frac{\alpha^2}{s^2t^2} \frac{1}{(s+u)} [(s^2+u^2)xF_1 + us(x2F_1 - F_2)] &= \sum_i f_i(x) x 2\pi \frac{\alpha^2 e_i^2}{t^2 s^2} \frac{s^2+u^2}{s+u} \\ \Leftrightarrow 2[(s^2+u^2)xF_1 + us(2xF_1 - F_2)] &= \sum_i x f_i(x) e_i^2 (s^2+u^2)\end{aligned}$$

Comparing the coefficients of $(s^2 + u^2)$ and $us$ provides the important formula of the parton model:

$$2xF_1 = F_2 = \sum_i x f_i(x) e_i^2 \tag{29}$$

The relation $F_L = F_2 - 2xF_1 = 0$ is the so called Callan-Gross relation, which is fullfilled in leading order of $\frac{1}{Q^2}$ [1]. We can see that in the leading order $F_1 = F_1(x)$ and $F_2 = F_2(x)$ are functions that depend only on the scaling variable $x$. The result is that important because the individual parton distribution functions now provide the overall structure of the proton or said differently, measuring the cross section of deep inelastic electron proton scattering provides information about how the parton structure of the proton looks like. The next section will deal with this fact in more detail.

### 3.3 Parton distribution functions (PDFs)

First, consider what the structure function $F_2$ would have to look like depending of the structure of the proton. The simplest possibility is if the proton consisted of only one quark. Then the entire proton momentum would be carried by this quark and $F_2$ would be a delta peak at 1. Looking at the properties of the proton (charge, spin, etc.), it can be assumed that the proton consists of three quarks. If these are not coupled with each other in the first consideration, $F_2$ would be a superposition of 3 delta peaks at 1/3, because each of the three quarks would then carry exactly 1/3 of the total momentum. If the three quarks can interact with each other, the momentum is no longer discrete but continuously distributed around the maximum at 1/3, the area is normalised to 1. This situation is visualised as a red curve in fig. 8. Here, the sum of the valence up and

down PDFs of the CT18 PDF sets with their uncertainties was plotted. The expected distribution can be seen clearly.
Now the idea of three valence quarks bound together is extended to include a sea of gluons and quark-antiquark pairs. The quarks and gluons in the sea carry only small momentum fractions. This idea is shown as a green curve in the figure. We can see that the curve no longer flattens out at small $x$. In a first approximation it is now

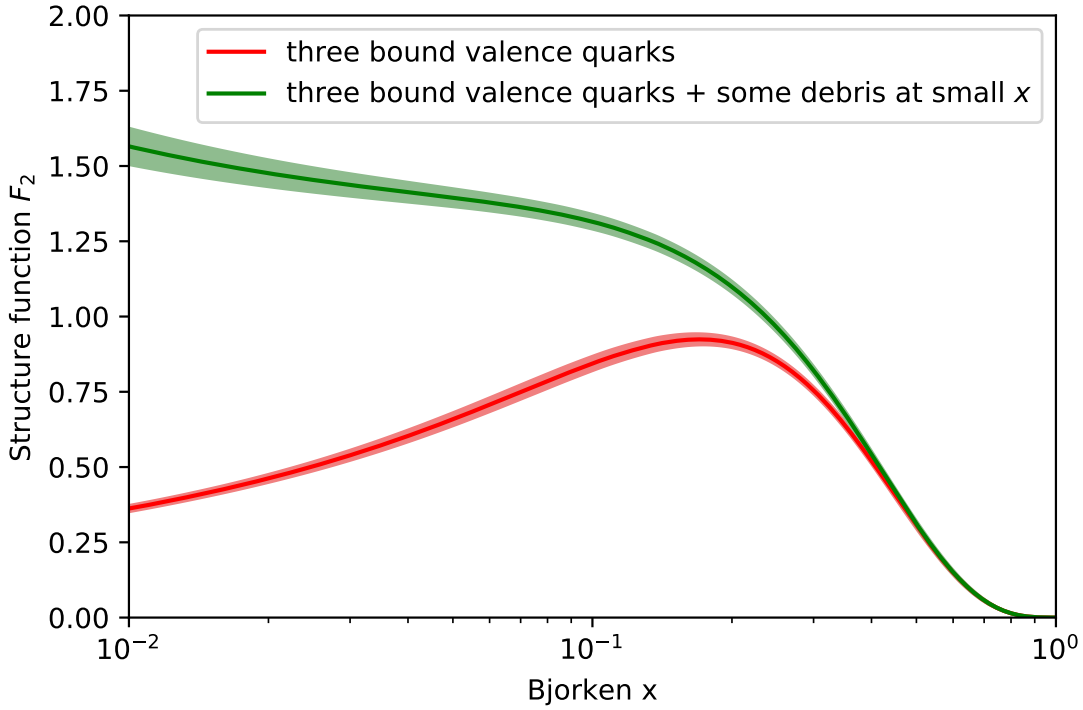


Figure 8: Structure function $F_2$ for three bounded valence quarks and in addition for three bounded valence quarks and a debris at small $x$ visualized with data from the CT18 PDF set.

assumed that the proton consists of up, down and strange quarks (and the respective antiparticles) and gluons, where the up quark has a charge of $\frac{2}{3}e$, the strange and the down quark each carry a charge of $-\frac{1}{3}e$. Furthermore we assume that the gluons just couple the quarks but do not carry a momentum fraction themselves. Then eq. (29) can be written in the form

$$\frac{1}{x}F_2 = \left(\frac{2}{3}\right)^2 [u^P(x) + \bar{u}^P(x)] + \left(\frac{1}{3}\right)^2 [d^P(x) + \bar{d}^P(x)] + \left(\frac{1}{3}\right)^2 [s^P(x) + \bar{s}^P(x)] \quad (30)$$

The functions $u^P$, $d^P$, $s^P$ or $\bar{u}^P$, $\bar{d}^P$, $\bar{s}^P$ are the distribution functions for (anti-)up, (anti-)down or (anti-)strange quarks. Thus, there are a total of 6 quark distribution functions $f_i(x)$ that are unknown. However, we know that the quantum numbers of

the proton are exactly the sum of the quantum numbers of the valence quarks, i.e. the quarks that are not in a quark-antiquark pair. The quantum numbers of the proton are: strangeness=0, electric charge=1, baryon number=1. Since only the strange quark can contribute to the strangeness, the following applies:

$$\int dx[s(x) - \bar{s}(x)] = 0$$

The strange quarks are therefore only present in quark-antiquark pairs. Since the up and down quarks each carry the baryon number $\frac{1}{3}$, the following also applies:

$$\int dx[u(x) - \bar{u}(x)] = 2$$
$$\int dx[d(x) - \bar{d}(x)] = 1$$

In order to visualize these facts, the valence parton distribution functions of the PDF sets that are mentioned in the introduction are shown in fig. 9.

To a first approximation, all seaquarks appear in the same number:

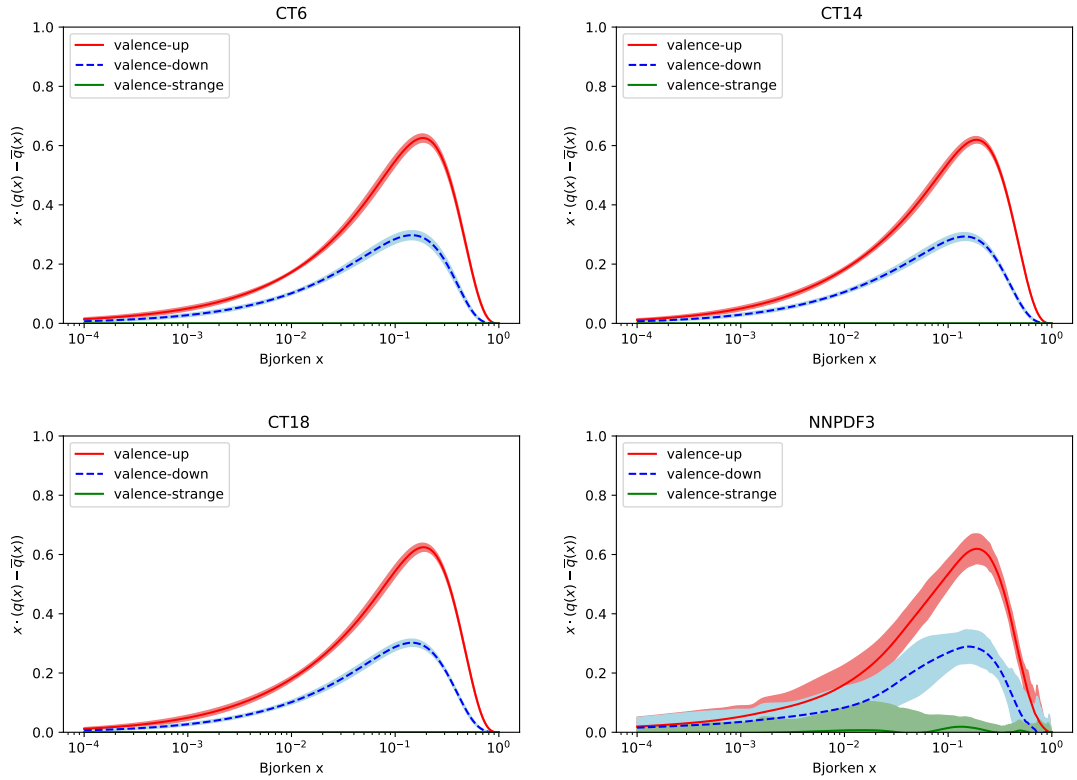


Figure 9: valence quark distribution for the PDF sets CTEQ6, CT14, CT18 and NNPDF3.

$$u_s = \bar{u}_s = d_s = \bar{d}_s = s_s = \bar{s}_s = S(x) \tag{31}$$

The valence quarks are those without antipartners, so we get:

$$u_v = u - \bar{u} = u - \bar{u}_s = u - u_s \tag{32}$$
$$d_v = d - \bar{d} = d - \bar{d}_s = d - d_s \tag{33}$$
$$s_v = 0 \tag{34}$$

Using these relations, in eq. (30) $u = u_v + S$ and $d = d_v + S$ can be substituted, resulting in

$$\frac{1}{x}F_2 = \frac{4}{9}u_v + \frac{1}{9}u_d + \frac{4}{3}S. \tag{35}$$

For the neutron, on the other hand, $\int dx[u(x) - \bar{u}(x)] = 1$ and $\int dx[d(x) - \bar{d}(x)] = 2$ to satisfy its quantum numbers and thus $\frac{1}{x}F_2^n = \frac{1}{9}u_v + \frac{4}{9}u_d + \frac{4}{3}S$. The subtraction of the two distribution functions yields

$$\frac{1}{f}(F_2 - F_2^n) = \frac{1}{3}(u_v - d_v)$$

and thus only the fraction of valence quarks, without the fraction of sea quarks. This is an example of how information about the quark content of the proton can be collected via a linear combination of structure functions of the proton during deep inelastic scattering with an electron.

The problem in determining the inner structure of the proton is obvious: At this point, the analysis of electron-proton scattering is no longer sufficient for general linear combinations of PDFs. Since the deep inelastic electron proton scattering is not sensitive to the individual strange or antistrange PDF we can not get information about the strange content in the proton. It is useful to consider deep inelastic scattering with neutrinos and antineutrinos to obtain more independent linear combinations of PDFs.

# 4 Weak interactions

The lifetimes of pions and muons are significantly longer than those of particles that decay through strong or electromagnetic interaction. This suggests that there must be another type of interaction that has a much weaker coupling than electromagnetism. This is the so-called weak interaction. All hadrons and leptons are subjected to it. Neutrinos can help out to observe a weak interaction process. These are subjected exclusively to the weak interaction, because they are colourless and electrically neutral, so that the weak interaction has to play a role in the neutrino quark scattering in any case.

### 4.1 Parity violation of weak interaction

In the most general form, the particle current can be described as

$$(\overline{\psi})(4 \times 4)(\psi).$$

The bracket $(4 \times 4)$ describes a general product of $\gamma$ matrices. It is significant how the individual constructions behave under space inversion, i.e. using the parity operator

$$\Lambda_P = \begin{pmatrix} 1 & 0 & 0 & 0 \\ 0 & -1 & 0 & 0 \\ 0 & 0 & -1 & 0 \\ 0 & 0 & 0 & -1 \end{pmatrix} \tag{36}$$

Under the condition that the parity transformation is a Lorentz transformation, it makes sense to consider the Dirac equation from eq. (A.2) in two systems $x$ and $x' = \Lambda_P x$ linked by parity

$$i\gamma^\mu \frac{\partial \psi(x)}{\partial x^\mu} - m\psi(x) = 0$$
$$i\gamma^\mu \frac{\partial \psi'(x')}{\partial x'^\mu} - m\psi(x') = 0.$$

Since both equations yield 0, there must be an operator for which $\psi'(x') = S\psi$ holds. If this is substituted into the lower equation, then in agreement with the upper equation $S^{-1}\gamma^\mu S = \Lambda_P \gamma^{mu}$ must hold. Substituting $\Lambda_P$ from eq. (36) concretely, we get $S^{-1}\gamma^0 S = \gamma^0$, and $S^{-1}\gamma^k S = -\gamma^k$. These relations are fulfilled exactly for $S = \gamma^0$. With this result and the relations from eq. (A.4), we can now consider which form of the current has which parity. This is summarised in table 2. Note that the construction $\gamma^5\gamma^\mu$ is effectively a

| form | parity | no. of components | phys. name |
|---|---|---|---|
| $\overline{\psi}\psi$ | | 1 | scalar |
| $\overline{\psi}\gamma^\mu\psi$ | $\gamma^0\overline{\psi}\gamma^\mu\psi = (-)\overline{\psi}\gamma^\mu\psi$ | 4 | Vector |
| $\overline{\psi}\sigma^{\mu\nu}\psi$ | | 6 | Tensor |
| $\overline{\psi}\gamma^5\gamma^\mu\psi$ | $\gamma^0\overline{\psi}\gamma^5\gamma^\mu\psi = (+)\overline{\psi}\gamma^5\gamma^\mu\psi$ | 4 | Axial Vector |
| $\overline{\psi}\gamma^5\psi$ | $\gamma^0\overline{\psi}\gamma^5\psi = (-)\overline{\psi}\gamma^5\psi$ | 1 | Pseudoscalar |

Table 2: Overview of the possibilities of constructions with $\gamma$-matrices [4]

product of 3 and not 5 $\gamma$ matrices, since two matrices are the same and the product can thus be reduced to 3. It can be stated about the tensor that it is antisymmetrical, i.e. in the form $\sigma^{\mu\nu} = \frac{1}{2}(\gamma^\mu\gamma^\nu - \gamma^\nu\gamma^\mu)$, since all symmetrical components fall out due to the anticommutator relation of the matrices. Therefore it also only has 6 independent components. The axial vector and the pseudoscalar appear strange because they look like a vector and a scalar in terms of the number of their components, but behave exactly

the opposite as expected when the parity operator is applied. When investigating the scattering experiments with electrons, the particle current was always described in the form of a vector, i.e. in such a way that it has the eigenvalue 1 when the parity operator is applied. This is what is to be expected from currents that can be observed in nature. Intuitively, it also seems nonsensical to describe the particle current in the form of an axial vector. However, a Priori, there is no reason to use only vectors to describe the particle currents. Replacing $\gamma^\mu$ by $\gamma^\mu(1-\gamma^5)$ has surprisingly lead to an explanation of a number of hitherto unexplained $\beta$-decay observations [4]. One speaks of the V-A structure (vector-axial vector) of the weak currents. The weak cross sections can therefore be calculated in the same way as those of the electromagnetic interaction by replacing $\gamma^\mu$ by $\frac{1}{2}\gamma^\mu(1-\gamma^5)$. The antisymmetric part of the neutrino current allows an antisymmetric fraction in the hadron tensor, which this time does not disappear due to the Gaussian summation convention.

### 4.2 Elastic electron-neutrino scattering

First, we investigate elastic electron-neutrino scattering. Later we will see that this calculation can be recycled for neutrino-quark scattering. To calculate the cross section

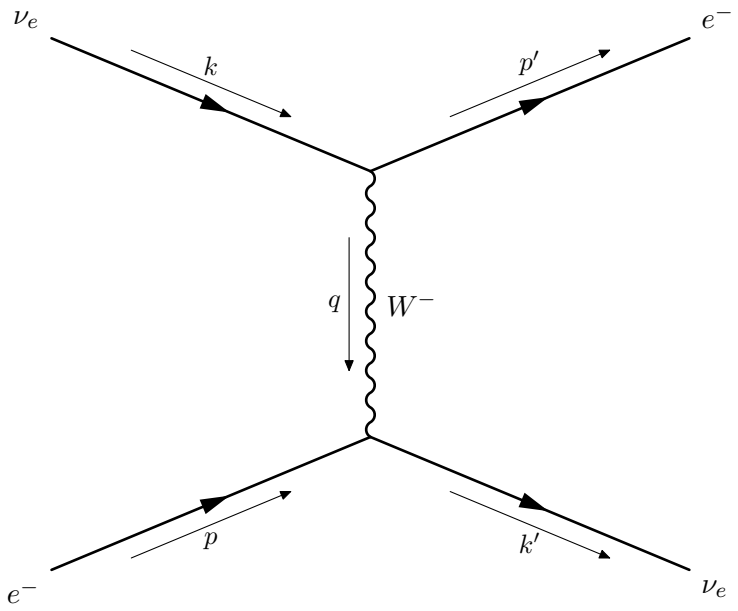


Figure 10: Feynman-diagram of electron-neutrino scattering [4]

of the electron-neutrino scattering, the Feynman diagram from fig. 10 is considered and we use the Feynman rules. We start the calculation of the effective cross-section at the

invariant amplitude.

$$M = [\frac{g}{\sqrt{2}}\bar{u}^{s_1}(k')\frac{1}{2}\gamma^\mu(1-\gamma^5)u^{s_2}(p)][\frac{g}{\sqrt{2}}\bar{u}^{s_3}(p')\frac{1}{2}\gamma_\mu(1-\gamma^5)u^{s_4}(k)]\underbrace{\frac{1}{Q^2+M_W^2}}_{\text{Propagator}}$$

Here $\frac{g}{\sqrt{2}}$ is a dimensionless weak coupling constant and $M_W$ the W-Boson mass. Assuming that $Q^2 \ll M_W^2$, then the propagator can be approximated as $\frac{1}{M_W^2}$.

$$\begin{aligned} M &= [\frac{g}{\sqrt{2}}\bar{u}^{s_1}(k')\frac{1}{2}\gamma^\mu(1-\gamma^5)u^{s_2}(p)][\frac{g}{\sqrt{2}}\bar{u}^{s_3}(p')\frac{1}{2}\gamma_\mu(1-\gamma^5)u^{s_4}(k)]\cdot \underbrace{\frac{1}{M_W^2}}_{\text{Propagator}} \\ &= \frac{g^2}{8}\underbrace{[\bar{u}^{s_1}(k')\gamma^\mu(1-\gamma^5)u^{s_2}(p)]}_{J_1^\mu}\underbrace{[\bar{u}^{s_3}(p')\gamma_\mu(1-\gamma^5)u^{s_4}(k)]}_{J_\nu^2}\frac{1}{M_W^2} \end{aligned} \tag{37}$$

In this case the weak interaction amplitudes are of the form

$$M = \frac{G_F}{\sqrt{2}}J_1^\mu J_\nu^2 \tag{38}$$

with

$$\frac{G_F}{\sqrt{2}} = \frac{g^2}{8M_W^2} \tag{39}$$

where $G_F$ is the Fermi constant [4]. So we get

$$\begin{aligned} M &= \frac{G_F}{\sqrt{2}}[\bar{u}^{s_1}(k')\gamma^\mu(1-\gamma^5)u^{s_2}(p)][\bar{u}^{s_3}(P')\gamma_\mu(1-\gamma^5)u^{s_4}(k)] \\ M^\dagger &= \frac{G_F}{\sqrt{2}}[u^{s_2\dagger}(p)(1-\gamma^5)^\dagger\gamma^{\nu\dagger}\bar{u}^{s_1\dagger}(k')][u^{s_4\dagger}(k)(1-\gamma^5)^\dagger\gamma_\nu{}^\dagger\bar{u}^{s_3\dagger}(p')] \\ &= \frac{G_F}{\sqrt{2}}[\bar{u}^{s_2}(p)\gamma^\nu(1-\gamma^5)u^{s_1}(k')][\bar{u}^{s_4}(k)\gamma_\nu(1-\gamma^5)u^{s_3}(p')] \end{aligned}$$

In contrast to the calculation of $\overline{|M|^2}$ for the electron-muon scattering in section 2.1 we can not multiply parts seperatly with each other. The multiplication and spin average

gives the following for the invariant amplitude

$$\begin{aligned}
\overline{|M|^2} &= \frac{1}{2}\sum_{s_1,s_2,s_3,s_4} MM^\dagger \\
&= \frac{G_F^2}{4}\mathrm{Tr}[\gamma^\mu(1-\gamma^5)\ \not{p}\gamma^\nu(1-\gamma^5)\ \not{k}']\mathrm{Tr}[\gamma_\mu(1-\gamma^5)\ \not{k}\gamma_\nu(1-\gamma^5)\ \not{p}'] \\
&= \frac{G_F^2}{4}p_\alpha k'_\beta[\mathrm{Tr}(\gamma^\mu\gamma^5\gamma^\alpha\gamma^\nu\gamma^5\gamma^\beta) + \mathrm{Tr}(\gamma^\mu\gamma^\alpha\gamma^\nu\gamma^\beta) \\
&\qquad - \mathrm{Tr}(\gamma^\mu\gamma^5\gamma^\alpha\gamma^\nu\gamma^\beta) - \mathrm{Tr}(\gamma^\mu\gamma^\alpha\gamma^\nu\gamma^5\gamma^\beta)] \\
&\quad \cdot k^\kappa p'^\lambda[\mathrm{Tr}(\gamma_\mu\gamma^5\gamma_\kappa\gamma^\nu\gamma^5\gamma^\lambda) + \mathrm{Tr}(\gamma^\mu\gamma^\kappa\gamma^\nu\gamma^\lambda) \\
&\qquad - \mathrm{Tr}(\gamma^\mu\gamma^5\gamma^\kappa\gamma^\nu\gamma^\lambda) - \mathrm{Tr}(\gamma^\mu\gamma^\kappa\gamma^\nu\gamma^5\gamma^\lambda)] \\
&= \frac{G_F^2}{4}2p_\alpha k'_\beta[\mathrm{Tr}(\gamma^\mu\gamma^\alpha\gamma^\nu\gamma^\beta) - \mathrm{Tr}(\gamma^\mu\gamma^5\gamma^\alpha\gamma^\nu\gamma^\beta)] \\
&\quad 2k^\kappa p'^\lambda[\mathrm{Tr}(\gamma_\mu\gamma_\kappa\gamma^\nu\gamma^\lambda) - \mathrm{Tr}(\gamma^\mu\gamma^5\gamma^\kappa\gamma^\nu\gamma^\lambda)] \\
&= \frac{G_F^2}{4}8p_\alpha k'_\beta[g^{\mu\alpha}g^{\nu\beta} - g^{\mu\nu}g^{\alpha\beta} + g^{\mu\beta}g^{\nu\alpha} + i\epsilon^{\mu\alpha\nu\beta}] \\
&\quad 8k^\kappa p'^\lambda[g_{\mu\kappa}g_{\nu\lambda} - g_{\mu\nu}g_{\kappa\lambda} + g_{\mu\lambda}g_{\nu\kappa} + i\epsilon^{\mu\kappa\nu\lambda}] \qquad (40)
\end{aligned}$$

Now the brackets must be multiplied. Note that the product of the $\epsilon$ tensors gives a product of $\delta$ functions as described in eq. (A.22). If we now put term by term together to form scalar products, we obtain:

$$\begin{aligned}
\overline{|M|^2} &= \frac{G_F^2}{4}64[(p\cdot k)(k'\cdot p') - \cancel{(p\cdot k')(k\cdot p')} + \cancel{(p\cdot p')(k\cdot k')} - \cancel{(k\cdot p')(p\cdot k')} \\
&\qquad + \cancel{4(p\cdot k')(k\cdot p')} - \cancel{(p\cdot k')(k\cdot p')} + \cancel{(k\cdot k')(p\cdot p')} - \cancel{(p\cdot k')(k\cdot p')} \\
&\qquad + (p\cdot k)(k'\cdot p') + 2(p\cdot k)(k'\cdot p') - \cancel{2(p\cdot p')(k\cdot k')}] \\
&= \frac{G_F^2}{4}\cdot 64\cdot 4(p\cdot k)(k'\cdot p') \\
&= G_F^2\cdot 64\cdot(p\cdot k)(k'\cdot p') \qquad (41)
\end{aligned}$$

If one also considers that in the CMS $s = (p+k)^2 = (p'+k')^2 = 2(p\cdot k) = 2(p'\cdot k')$ applies if one neglects the masses of the particles, then we get

$$\overline{|M|^2} = 16\cdot G_F^2\cdot s^2 \qquad (42)$$

The effective cross section can again be calculated via eq. (3). The initial flux $F$ results from the consideration in the CMS, where $|\vec{k}| = |\vec{p}| = p_i$, according to eq. (A.14) to $F = 4(p_iE_p + p_iE_k) = 4p_i\sqrt{s}$. The invariant phase space element can be obtained from

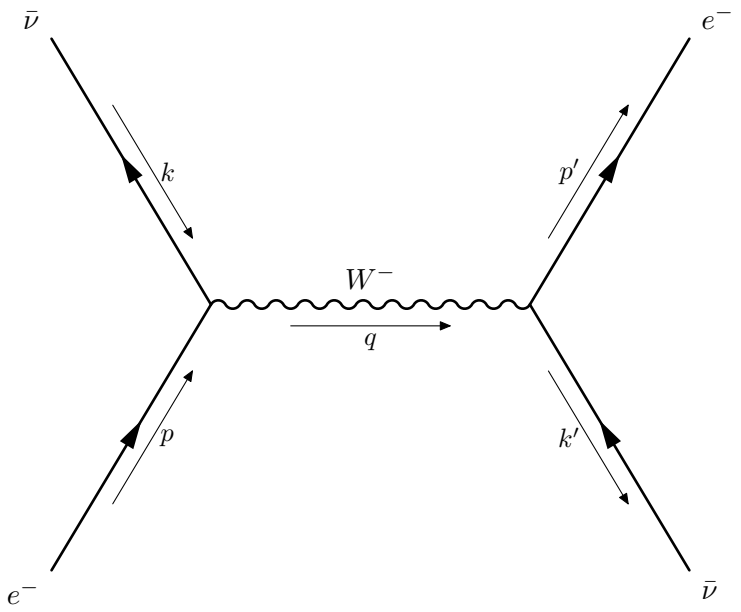


Figure 11: Feynman diagram of electron-antineutrino scattering.

eq. (A.21). In total we obtain:

$$\begin{aligned}\frac{d\sigma}{d\Omega} &= \frac{1}{4p_i\sqrt{s}}\frac{1}{4\pi^2}\frac{p_f}{4\sqrt{s}}\cdot 16G_F^2\cdot s^2 \\ &= \frac{G_F^2\cdot s}{4\pi^2}\frac{p_f}{p_i} \\ &= \frac{G_F^2\cdot s}{4\pi^2}\end{aligned}$$

Here, in the limit $m_e \to 0$, it was exploited that $p_f = p_i$ applies. After integration over the solid angle, the result is:

$$\sigma = \frac{G_F^2\cdot s}{\pi} \tag{43}$$

Figure 11 shows the Feynman diagram for electron-antineutrino scattering. The effective cross section can be obtained directly from that of electron-neutrino scattering. This can be recognised by the fact that the antineutrino can be regarded as a neutrino with reversed momentum, so $k \leftrightarrow -k'$. Substituting in eq. (41) yields

$$\overline{|M|^2} = G_F^2\cdot 64\cdot (p\cdot k')(k\cdot p') \tag{44}$$

for the invariant amplitude in antineutrino-electron scattering. The scattering angle $\theta$ is defined as the angle between the (anti)neutrino momentum before ($k$) and the electron

after ($p'$) scattering. So here

$$u \approx -2(k \cdot p') = -2(k' \cdot p) = -\frac{1}{2}s(1 - \cos\theta).$$

We get

$$\overline{|M|^2} = 16 \cdot G_F^2 \cdot u^2 = 4G_F^2 \cdot s^2(1 - \cos\theta)^2.$$

In this case, the effective cross section is

$$\begin{aligned}\left(\frac{d\sigma}{d\Omega}\right)_{\text{Antineutrino}} &= \frac{G_F^2 \cdot u^2}{4\pi^2 s} \\ &= \frac{G_F^2 \cdot s}{16\pi^2}(1 - \cos\theta)^2. \end{aligned} \tag{45}$$

The angular integration provides

$$\sigma_{\text{Antineutrino}} = \frac{G_F^2 \cdot s}{3\pi} = \frac{1}{3}\sigma_{\text{Neutrino}} \tag{46}$$

This result can be checked experimentally and thus confirm the form $\gamma^\mu(1 - \gamma^5)$ of the weak interaction vertex. Looking at eq. (45), we see that backscattering (i.e. $\theta = 0$) is forbidden in electron-antineutrino scattering. This can be explained by the fact that the helicity does not change for the two particles. With the backscattering, however, the momentum would rotate and thus the angular momentum would also have to rotate in order to maintain the helicity. Thus, an angular momentum state $J = 1$ would become a state with $J = -1$, which is forbidden according to the conservation of angular momentum. Strictly speaking, this scattering always ends in a state with $J = 1$ and a helicity of $+1$, so that only one of the three possible helicity states is assumed for the total system of the two particles. Thus, according to these symmetry considerations, the scattering amplitude is proportional to the element $d_1^{-1,1}(\Theta) = \frac{1}{2}(1 - \cos\Theta)$ of the Wigner-d matrix, which coincides with our result on the cross section.

### 4.3 (anti-)neutrino-quark scattering

In order to calculate the effective cross section of neutrino-quark scattering, we need to know what the weak quark currents look like. The quarks behave electromagnetically like leptons with their individual charge fraction. The weak current can therefore be constructed in the same way as for leptons.

$$J_q^\mu = \overline{u_q}\gamma^\mu(1 - \gamma^5)u_{q'} \tag{47}$$

When a neutrino hits the nucleon, all but one quarks are pure „observer quarks“, which means that the scattering effectively takes place on one particle. The Feynman diagram for this process for the scattering on a strange quark with a muonic neutrino is shown in fig. 12. The weak interaction can only couple to left-handed quarks, i.e. at very

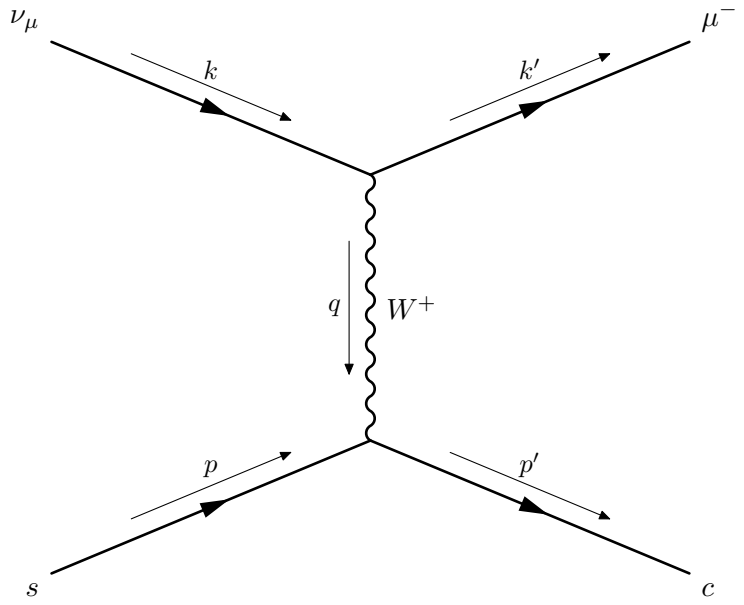


Figure 12: Feynman diagram of neutrino-quark scattering.

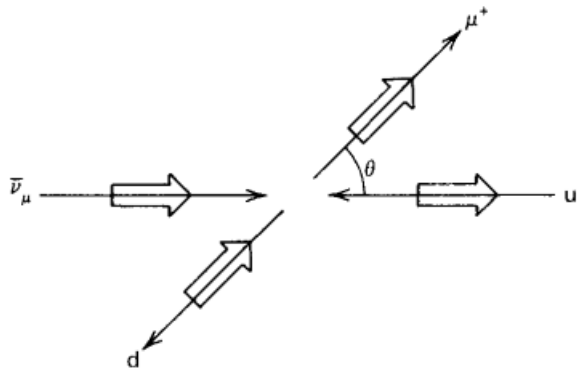


Figure 13: Helicity and angular configuration in antineutrino quark scattering [4].

high energies only to quarks with negative helicity. The cross section for scattering with a neutrino and an antineutrino can be taken from the calculation of electron-neutrino scattering. However, the scattering angle is now defined as shown in fig. 13. We obtain:

$$\left(\frac{d\sigma}{d\Omega}\right)_{\nu_\mu d\to\mu^- u} = \frac{G_F^2 \cdot s}{4\pi^2}$$
$$\left(\frac{d\sigma}{d\Omega}\right)_{\overline{\nu}_\mu u\to\mu^+ d} = \frac{G_F^2 \cdot s}{16\pi^2}(1-\cos(\theta+\pi))^2 = \frac{G_F^2 \cdot s}{16\pi^2}(1+\cos\theta)^2$$

With the help of the variable $y$ from eq. (18), the integration via $d\Omega$ can be replaced. We use the relation

$$1 - y = \frac{p\cdot k'}{p\cdot k} = \frac{1}{2}(1+\cos\theta)$$

in the CMS, to replace $d\Omega = 4\pi dy$ and $1+\cos\theta = 2(1-y)$. In addition, one proceeds to $s \to xs$, since each quark only carries the fraction $x$ of the total momentum. Thus, the two cross sections for the parton $i$ result in

$$\left(\frac{d\sigma_i}{dy}\right)_{\nu_\mu d\to\mu^- u} = \frac{G^2 xs}{\pi} = \left(\frac{d\sigma_i}{dy}\right)_{\bar{\nu}_\mu \bar{d}\to\mu^+\bar{u}} \tag{48}$$
$$\left(\frac{d\sigma_i}{dy}\right)_{\overline{\nu}_\mu u\to\mu^+ d} = \frac{G^2 xs}{\pi}(1-y)^2 = \left(\frac{d\sigma_i}{dy}\right)_{\nu_\mu \overline{u}\to\mu^-\overline{d}}$$

Note that the cross section for the process $\nu_\mu \overline{u} \to \mu^- \overline{d}$ is also that of the second line by inversion.

### 4.4 Parton formula for weak interactions

Equivalently to eq. (27), the total effective cross section of neutrino-proton scattering is to be represented by the individual neutrino-quark cross sections, which can be expressed by the equation

$$\left(\frac{d\sigma}{dxdy}\right)_{\nu P\to\mu X} = \sum_i f_i(x)\left(\frac{d\sigma_i}{dy}\right) \tag{49}$$

In order to find a connection to the form factors of the proton, the cross section of the neutrino-proton scattering will be calculated. Using eq. (38), the amplitude is of the form

$$\overline{|M|^2} = \frac{G_F^2}{2} W^{\mu\nu} L_{\mu\nu}^{\text{neutrino}}. \tag{50}$$

First we calculate $L_{\mu\nu}^{\text{neutrino}}$:

$$\begin{aligned} L_{\mu\nu}^{\text{neutrino}} &= \frac{1}{2}\sum_{s_1,s_2}[\bar{u}(k')^{s_1}\gamma^\mu(1-\gamma^5)u^{s_2}(k)][\bar{u}(k')^{s_1}\gamma^\mu(1-\gamma^5)u^{s_2}(k)]^\dagger \\ &= (-g_{\mu\nu}(k\cdot k') + k_\mu k'_\nu + k_\nu k'_\mu + i\epsilon_{\mu\nu\rho\sigma}k^\rho k'^\sigma) \end{aligned} \tag{51}$$

We see the appearance of an additional antisymmetric term as noted before. So we now need the additional antisymmetric term with the structure factor $W_3$, which was saved up, in the proton tensor.

$$W^{\mu\nu} = W_1(-g^{\mu\nu} + \frac{q^\mu q^\nu}{q^2}) + \frac{W_2}{M^2}(p^\mu - \frac{q\cdot p}{q^2}q^\mu)(p^\nu - \frac{q\cdot p}{q^2}q^\nu) + i\frac{W_3}{M^2}\epsilon^{\mu\nu\kappa\lambda}p_\kappa q_\lambda \tag{52}$$

We can multiply the two antisymmetric parts as follows:

$$\begin{aligned} W^{\mu\nu}_{\text{antisymm.}} L^{\text{neutrino}}_{\mu\nu\ \text{antisymm.}} &= \frac{i}{M^2} W_3 \epsilon^{\mu\nu\kappa\lambda} p_\kappa q_\lambda \cdot i\epsilon_{\mu\nu\rho\sigma} k^\rho k'^\sigma \\ &= \frac{1}{M^2} W_3 p_\kappa q_\lambda k^\rho k'^\sigma 2[\delta^\kappa_\rho \delta^\lambda_\sigma - \delta^\kappa_\sigma \delta^\lambda_\rho] \\ &= \frac{2}{M^2} W_3 [(p\cdot k)(q\cdot k') - (p\cdot k')(q\cdot k)] \end{aligned}$$

At this point we use $q = (k - k')$ to replace $q$.

$$\begin{aligned} W^{\mu\nu}_{\text{antisymm.}} L^{\text{neutrino}}_{\mu\nu\ \text{antisymm.}} &= \frac{2}{M^2} W_3 [(p\cdot k)(k\cdot k' - \underbrace{k'^2}_{=0}) - (p\cdot k')(\underbrace{k^2}_{=0} - k'\cdot k)] \\ &= \frac{2}{M^2} W_3 (k\cdot k')[(p\cdot k) + (p\cdot k')] \\ &\underbrace{=}_{\text{CMS}} \frac{2}{M^2} W_3 EE'(1-\cos\theta))(ME + ME') \\ &= \frac{4}{M} W_3 EE'(E+E')\sin^2\frac{\theta}{2} \end{aligned} \tag{53}$$

The product of the symmetrical parts can be recycled from the electron-muon scattering calculation (eq. (22)) with the additional factor $\frac{1}{4}$. In total we get

$$L^{\text{neutrino}}_{\mu\nu} W^{\mu\nu} = 4EE'(2W_1 \sin^2\frac{\theta}{2} + W_2 \cos^2\frac{\theta}{2} + \frac{W_3}{M}(E+E')\sin^2\frac{\theta}{2})$$

Using the relations for $Q^2$ and $xy$ of eq. (A.9) and eq. (A.11), we can replace $\sin^2\frac{\theta}{2} = xy\frac{M}{2E'}$ and $\cos^2\frac{\theta}{2} = \frac{E}{E'}(1 - y - xy\frac{M}{2E})$. We also replace $W_1$ and $W_2$ by $F_1$ and $F_2$ as we did in eq. (24) and $W_3 = \frac{F_3}{v} = \frac{E}{yE}$:

$$\begin{aligned} L^{\text{neutrino}}_{\mu\nu} W^{\mu\nu} &= 4EE'\left(\frac{xy}{E'}F_1 + \frac{1}{yE'}(1 - y - xy\frac{M}{2E})F_2 + \frac{1}{E'}(1-\frac{y}{2})xF_3\right) \\ &= 4E\left(xyF_1 + \frac{1}{y}(1 - y - xy\frac{M}{2E})F_2 + (1-\frac{y}{2})xF_3\right) \end{aligned} \tag{54}$$

With the normalisation $16\pi M$ and eq. (38) we obtain for the invariant amplitude:

$$\overline{|M|^2} = 32G_F^2\pi ME\left(xyF_1 + \frac{1}{y}(1 - y - xy\frac{M}{2E})F_2 + (1-\frac{y}{2})xF_3\right) \tag{55}$$

Now we can calculate the total cross section using eq. (3), eq. (A.16) and eq. (A.17).

$$d\sigma = \underbrace{\frac{1}{4ME}}_{F} \underbrace{\frac{E'dE'd\Omega}{2(2\pi)^3}}_{dQ} \underbrace{32G_F^2\pi ME\left(xyF_1 + \frac{1}{y}(1-y-xy\frac{M}{2E})F_2 + (1-\frac{y}{2})xF_3\right)}_{\overline{|M|^2}}$$
$$= G_F^2\frac{E'}{2\pi^2}\left(xyF_1 + \frac{1}{y}(1-y-xy\frac{M}{2E})F_2 + (1-\frac{y}{2})xF_3\right)dE'd\Omega$$

If we remember that the result is to be inserted into eq. (49) for comparison, it makes sense to switch to $dxdy$.We use eq. (A.12) and eq. (A.10):

$$d\sigma = G_F^2\frac{E'}{2\pi^2}\left(xyF_1 + \frac{1}{y}(1-y-xy\frac{M}{2E})F_2 + (1-\frac{y}{2})xF_3\right)\frac{2\pi ME}{E'}ydxdy$$
$$= G_F^2\frac{ME}{\pi}\left(xy^2F_1 + (1-y-xy\frac{M}{2E})F_2 + y(1-\frac{y}{2})xF_3\right)dxdy \tag{56}$$

For a coefficient comparison in powers of $s$, $u$ and $t$ in the formula eq. (49) we use:

$$y = 1 + \frac{u}{s},$$
$$ME = \frac{1}{2}s$$

in eq. (56) and we neglect the part with $xy\frac{M}{2E}$ in the extreme relativistic limit, like we did when we derived eq. (29). Since $E = \frac{Q^2}{2Mxy}$ from eq. (A.11) and in the limit $M^2 \ll Q^2$ or $\frac{M^2}{Q^2} \to 0$ the part is negligible. We get:

$$\frac{d\sigma}{dxdy} = \frac{G_F^2}{2\pi}\left(\frac{x(s+u)^2}{s}F_1 - uF_2 + \frac{1}{2}x(s-\frac{u^2}{s})F_3\right)$$
$$= \frac{G_F^2}{2\pi}\left(xs(F_1 + \frac{1}{2}F_3) + u(2xF_1 - F_2) + x\frac{u^2}{s}(F_1 - \frac{1}{2}F_3)\right) \tag{57}$$

We can insert eq. (57) and eq. (48) into eq. (49):

$$\frac{G_F^2}{2\pi}\left(xs(F_1 + \frac{1}{2}F_3) + u(2xF_1 - F_2) + x\frac{u^2}{s}(F_1 - \frac{1}{2}F_3)\right) = \frac{G_F^2xs}{\pi}\sum_{i,k}\left(f_i(x) + \frac{u^2}{s^2}f_k(x)\right)$$
$$\Leftrightarrow \left(xs(2F_1 + F_3) + 2u(2xF_1 - F_2) + x\frac{u^2}{s}(2F_1 - F_3)\right) = \sum_{i,k}\left(4xsf_i(x) + 4x\frac{u^2}{s}f_k(x)\right)$$

Here $f_i(x)$ are the structure functions of quarks, which interact with the neutrino and $f_k(x)$ are the structure functions of the antiquarks, which interact with the neutrino. The comparison of coefficients provides:

$$\begin{array}{lll} (i) & 2xF_1 = F_2 & \underbrace{\Longrightarrow F_L = F_2 - 2xF_1 = 0}_{\text{Callan-Gross relation}} \\ (ii) & 2xF_1 + xF_3 = 4\sum_i f_i(x)x & \\ (iii) & 2xF_1 - xF_3 = 4\sum_k f_k(x)x & \end{array} \tag{58}$$

First we see in (i) that the deep inelastic proton neutrino structure functions still satisfy the Callan-Gross relation, which were also fulfilled in electron proton scattering [1]. It should be noted that (i) is an approximated solution, since the part with prefactor $xy\frac{M}{2E}$ was neglected in the coefficient comparison. In fact $F_L$ is not 0 zero but it is small. Adding and subtracting the last two lines yields:

$$\begin{aligned}\frac{1}{2}[(ii)-(iii)]: \quad & F_3 = 2\left(\sum_i f_i(x) - \sum_k f_k(x)\right)\\ \frac{1}{2}[(ii)+(iii)]: \quad & \frac{F_2}{x} = 2\left(\sum_i f_i(x) + \sum_k f_k(x)\right)\end{aligned} \tag{59}$$

where line $(i)$ was used to substitute $F_1$. From these equations, linear combinations can now be formed, which can produce a wide variety of PDFs. If we look at the scattering at a target consisting of equal numbers of protons and neutrons, we can, by taking advantage of the fact that in a neutron the number of u- and d-quarks and antiquarks are swapped in contrast to the proton, use

$$\begin{aligned}d(x) + d^n(x) &= d(x) + u(x) \equiv Q(x)\\ \overline{u}(x) + \overline{u^n}(x) &= \overline{u}(x) + \overline{d}(x) \equiv \overline{Q}(x).\end{aligned} \tag{60}$$

The scattering of the u and d quarks of the proton (which are a first approximation of the quark content) is thus described by the scattering of the d quarks at the entire target, the scattering of the anti-u and anti-d quarks of the proton (which is in a first approximation the antiquark content) by that of the scattering of the anti-u quarks of the entire target. This fact inserted into eq. (59) yields

$$\left(\frac{d\sigma}{dxdy}\right)_{\nu P\to\mu^- X} = \frac{G_F^2 sx}{2\pi}(Q(x) + (1-y)^2\overline{Q}(x))$$

and in equivalence

$$\left(\frac{d\sigma}{dxdy}\right)_{\overline{\nu} P\to\mu^+ X} = \frac{G_F^2 sx}{2\pi}(\overline{Q}(x) + (1-y)^2 Q(x)).$$

From these two equations, the quark content $Q$ and the antiquark content $\overline{Q}$ of the proton can be separated, which means that the fraction of quarks and antiquarks in a first approximation where the proton just consists of (anti)up and (anti)down quarks can be determined from the measurement of the two cross sections.

### 4.5 Linear combinations for strange quark content

In the following, the proton consisting of (anti)up, (anti)down and (anti)strange quarks is considered. The neutrino can interact via charged current with $d$, $s$ and $\overline{u}$, so we get

$$\begin{aligned}F_3^\nu &= 2[s + d - \overline{u}],\\ \frac{F_2^\nu}{x} &= 2[s + d + \overline{u}].\end{aligned} \tag{61}$$

This result, neglecting the charm quark distribution, is consistent with the structure functions from [8]. In contrast to that the antineutrino interact with $\overline{d}$, $\overline{s}$ and $u$ quarks, so in the case of antineutrino proton scattering we get

$$\begin{aligned} F_3^{\bar{\nu}} &= 2[u - \overline{s} - \overline{d}], \\ \frac{F_2^{\overline{\nu}}}{x} &= 2[u + \overline{s} + \overline{d}]. \end{aligned} \tag{62}$$

It is easy to see, that

$$\begin{aligned} F_2^{\nu} + F_2^{\overline{\nu}} &= 2x \sum_i (q_i + \bar{q}_i) \\ F_3^{\nu} + F_3^{\overline{\nu}} &= 2(s + d - \overline{u} - \overline{s} - \overline{d} + u) = 2(u_v + d_v). \end{aligned}$$

For an isoscalar target $N$, where the number of protons and neutrons are equal (and therefore the number of $u$ and $d$ quarks and $\overline{u}$ and $\overline{d}$ quarks) we get

$$\begin{aligned} F_2^{N,\nu} &= 2x \left[ \frac{s + \overline{s}}{2} + \frac{u + d}{2} + \frac{\overline{u} + \overline{d}}{2} \right] = x \sum_i (q_i + \overline{q_i}) = F_2^{N,\overline{\nu}} \\ F_3^{N,\nu} &= 2 \left[ \frac{s + \overline{s}}{2} + \frac{u + d}{2} - \frac{\overline{u} + \overline{d}}{2} \right] = (u_V + d_V) + (s + \overline{s}) \\ F_3^{N,\overline{\nu}} &= (u_V + d_V) - (s + \overline{s}). \end{aligned} \tag{63}$$

Here we used $u_v = u - \bar{u}$ and $d_v = d - \overline{d}$. It makes sense to consider the following linear combinations:

$$\begin{aligned} F_3^{N,\nu} - F_3^{N,\overline{\nu}} &= 2(s + \overline{s}) \\ F_2^{N,\nu} - F_3^{N,\nu} &= 2(\overline{u} + \overline{d}) \end{aligned}$$

So we get the following expression for the strange content of proton quark sea

$$R_s = \frac{s + \overline{s}}{\overline{u} + \overline{d}} = \frac{F_3^{N,\nu} - F_3^{N,\overline{\nu}}}{F_2^{N,\nu} - F_3^{N,\nu}} \tag{64}$$

In addition the neutrino and antineutrino cross sections allow a determination of both, $s$ and $\overline{s}$ separately.

# 5 Dimuon production

One method of determining the strange content of the proton is to measure the ratio of dimuon to charged current cross section. The NOMAD experiment measures the ratio

$$R_{\mu\mu} = \frac{\sigma_{\mu\mu}}{\sigma_{cc}} \tag{65}$$

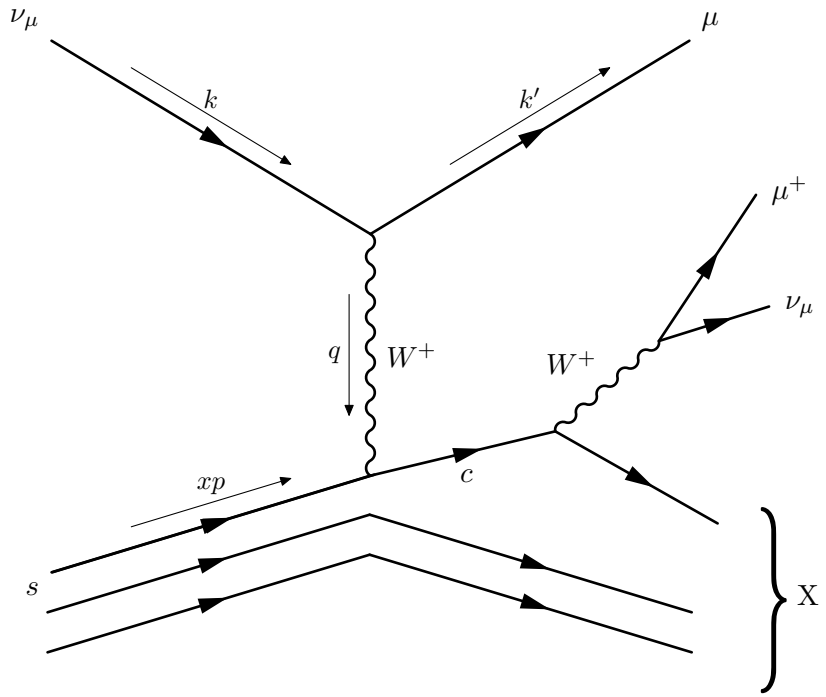


Figure 14: Feynman-diagram of charmed dimuon production

The Feynman diagram of the process of charm induced dimuon production is shown in fig. 14. When the incident neutrino scatters with a strange quark (or, also possible but less probable as we will see, with a down quark), a charm quark is created, which forms a charmed hadron. In a further step, this decays into a strange or down quark, a neutrino and a muon. Together with the first muon from the neutrino scattering, two muons can be detected. The use of the ratio allows a reduction to few uncertainties, as uncertainties that occur in both the numerator and the denominator are dropped out. These include, for example, the uncertainties from the incident neutrino current, which is very large and thus the ignorance about it can be avoided. The systematic uncertainties for the ratio are smaller than 2% and smaller than the statistical uncertainties [7].

## 5.1 Charged current cross section

In order to be able to interpret the experimental results, we need a non-approximated form of the cross section for neutrino-proton charged current scattering $\sigma_{cc}$. At this point we no longer want to approximate the propagator to $\frac{1}{M_W^2}$ but replace it with the correct value of $\frac{1}{M_W^2+Q^2}$. Therefore, we get the factor $\frac{M_W^4}{(M_W^2+Q^2)^2} = \frac{1}{(1+\frac{Q^2}{M_W^2})^2}$ and we

insert this in eq. (56):

$$\sigma_{cc} = \frac{G_F^2 ME}{\pi} \frac{1}{(1+\frac{Q^2}{M_W^2})^2} \left( xy^2 F_1^\nu + (1 - y - xy\frac{M}{2E}) F_2^\nu + y(1-\frac{y}{2}) x F_3^\nu \right) dxdy$$

With $xy = \frac{Q^2}{2ME}$ we can use $dy = \frac{1}{2MEx} dQ^2$.

$$\begin{aligned}
\sigma_{cc} &= \frac{G_F^2}{2\pi x} \frac{1}{(1+\frac{Q^2}{M_W^2})^2} \left( xy^2 F_1^\nu + (1 - y - xy\frac{M}{2E}) F_2^\nu + y(1-\frac{y}{2}) x F_3^\nu \right) dxdQ^2 \\
&= \frac{G_F^2}{2\pi(1+\frac{Q^2}{M_W^2})^2 x} \cdot \\
&\left( \frac{1}{2} y^2 \underbrace{(2xF_1^\nu - F_2^\nu)}_{=-F_L^\nu} + \underbrace{(1 - y + \frac{1}{2}y^2}_{=\frac{1}{2}Y_+} - xy\frac{M}{2E}) F_2^\nu + \underbrace{(y - \frac{y^2}{2}}_{=\frac{1}{2}Y_-}) x F_3^\nu \right) dxdQ^2
\end{aligned}$$

We use $F_L^\nu = F_2^\nu - 2xF_1^\nu$, $Y_\pm = 1 \pm (1-y)^2$ as indicated in the formula.

$$\frac{d\sigma_{cc}}{dQ^2 dx} = \frac{G_F^2}{4\pi(1+\frac{Q^2}{M_W^2})^2 x} \left( (Y_+ - \frac{2x^2y^2M^2}{Q^2}) F_2^\nu - y^2 F_L^\nu + Y_- x F_3^\nu \right)$$

$F_2$ and $F_3$ are the structure functions from eq. (61), since we approximate that the proton momentum is carried only by (anti)up, (anti)down and (anti)strange quarks. We assume the Callan-Gross relation $F_L = 0$ and evaluate the cross section in the limit $\frac{M^2}{Q^2} \to 0$ so the cross section becomes

$$\frac{d\sigma_{cc}}{dQ^2 dx} = \frac{G_F^2}{4\pi(1+\frac{Q^2}{M_W^2})^2 x} \left( Y_+ F_2^\nu + Y_- x F_3^\nu \right).$$

The NOMAD experiment measures the ratio for an iron target, which is approximately an isoscalar target. Therefore the cross section is

$$\frac{d\sigma_{cc}^N}{dQ^2 dx} = \frac{G_F^2}{4\pi(1+\frac{Q^2}{M_W^2})^2 x} \left( Y_+ F_2^{\nu,N} + Y_- x F_3^{\nu,N} \right). \tag{66}$$

with

$$\begin{aligned}
F_2^\nu &= x \sum_i (q_i + \overline{q}_i) \\
F_3^\nu &= (u_V + d_V) + (s + \overline{s})
\end{aligned}$$

from eq. (63). Equation (66) is an expression for the cross section of charged current neutrino-proton scattering. In the following we want to derive the cross section for charm dimuon production $\sigma_{\mu\mu}$.

## 5.2 Dimuon production cross section

In order to derive the charm dimuon production cross section we start with the general charged current cross section for neutrino-proton scattering from eq. (66):

$$\frac{\sigma_{cc}}{dQ^2dx} = \frac{G_F^2}{4\pi x(1+\frac{Q^2}{M_W^2})^2}\left(Y_+F_2 + Y_-xF_3\right)$$

Here $F_i$ with i=2, L, 3 are the structure functions of the proton for the charged current cross section. We know that only $d$ and $s$ quarks can convert to a charm quark via charged current weak interaction. Thus we obtain from eq. (61) the structure functions of the proton for dimuon production

$$xF^{\nu}_{3,\mu\mu} = F^{\nu}_{2,\mu\mu} = 2x\left[|V_{cs}|^2 s(x) + |V_{cd}|^2 d(x)\right] \tag{67}$$

Here $|V_{cs}|^2$ and $|V_{cd}|^2$ are the matrix elements of the 2x2 CKM Matrix [4].

$$\begin{bmatrix} |V_{ud}| \approx 0,973 & |V_{us}| \approx 0,23 \\ |V_{cd}| \approx 0,24 & |V_{cs}| \approx 0,97 \end{bmatrix}$$

s The strange quark contribution dominates the charm production at small $x$, since $|V_{cd}| \ll |V_{cs}|$. For an isoscalar target the term becomes

$$F^{\nu,N}_{2,\mu\mu} = 2x\left[|V_{cs}|^2 s(x) + |V_{cd}|^2 \frac{d(x)+u(x)}{2}\right] = xF^{\nu,N}_{3,\mu\mu} \tag{68}$$

Furthermore, the effective semileptonic branching ratio $B_\mu$ must be considered, which takes into account the probability of the muonic decay of the hadron. $B_\mu$ is of the form

$$B_\mu = \frac{a}{1+\frac{b}{E_\nu}}.$$

The free parameters $a$ and $b$ can be determined with a fit for the NOMAD data and the result is $a = (0.097 \pm 0.003)$ and $b = (6.7 \pm 1.8)$ GeV [7]. In summary, we obtain for the cross section of the dimuon production the approximated result

$$\begin{aligned}
\frac{\sigma_{\mu\mu}}{dQ^2dx} &= \frac{G_F^2}{4\pi x(1+\frac{Q^2}{M_W^2})^2}\cdot\left(Y_+F_{2,\mu\mu} + Y_-xF_{3,\mu\mu}\right)B_\mu \\
&= \frac{G_F^2}{4\pi x(1+\frac{Q^2}{M_W^2})^2}(2\cdot 2x)\left[|V_{cs}|^2 s(x) + |V_{cd}|^2\frac{d(x)+u(x)}{2}\right]\cdot B_\mu \\
&= \frac{G_F^2}{\pi x(1+\frac{Q^2}{M_W^2})^2}\cdot x\cdot\left[|V_{cs}|^2 s(x) + |V_{cd}|^2\frac{d(x)+u(x)}{2}\right]\cdot B_\mu
\end{aligned} \tag{69}$$

### 5.3 Calculation of the NOMAD ratio and comparison with measured data

Both the nominator $\sigma_{\mu\mu}$ and the denumerator $\sigma_{CC}$ of the NOMAD ratio $R_{\mu\mu}$ can be calculated from the differential cross sections using a double integral. It must be noted that $x$ and $Q^2$ are linked with each other via the relation $Q^2 = 2MExy$. Since we know that $y < 1$, the maximal value for $Q^2$ is $Q^2_{\text{max}}(x) = 2MEx$. There is also a minimal value for $Q^2$ because deep inelastic scattering can only be assumed from a certain momentum transfer onwards. It is usual to choose $Q^2_{\text{min}} = 1$ GeV$^2$ [3]. This also directly provides a minimum value for $x$, namely $x_{\text{min}} = \frac{Q^2_{\text{min}}}{2ME}$. We get

$$\sigma_{\mu\mu/CC}(E_\nu) = \int_{x_{\text{min}}}^{1} \int_{Q^2_{\text{min}}}^{Q^2_{\text{max}}(x)} \frac{d\sigma_{\mu\mu/CC}(E_\nu)}{dxdQ^2} dxdQ^2 \tag{70}$$

First, let us compare the inclusive charged current cross section $\sigma_{CC}$ with existing data from the NOMAD detector. In fig. 15, the measured values for $\sigma_{CC}$ are plotted against the neutrino energy. The measured values were taken from [9]. The plot was calculated with the help of eq. (70) in the leading-order. The PDFs of the NNPDF3 set were used for this purpose [3]. The energy range of $E_\nu < 30$ GeV is dominated by quasi-elastic

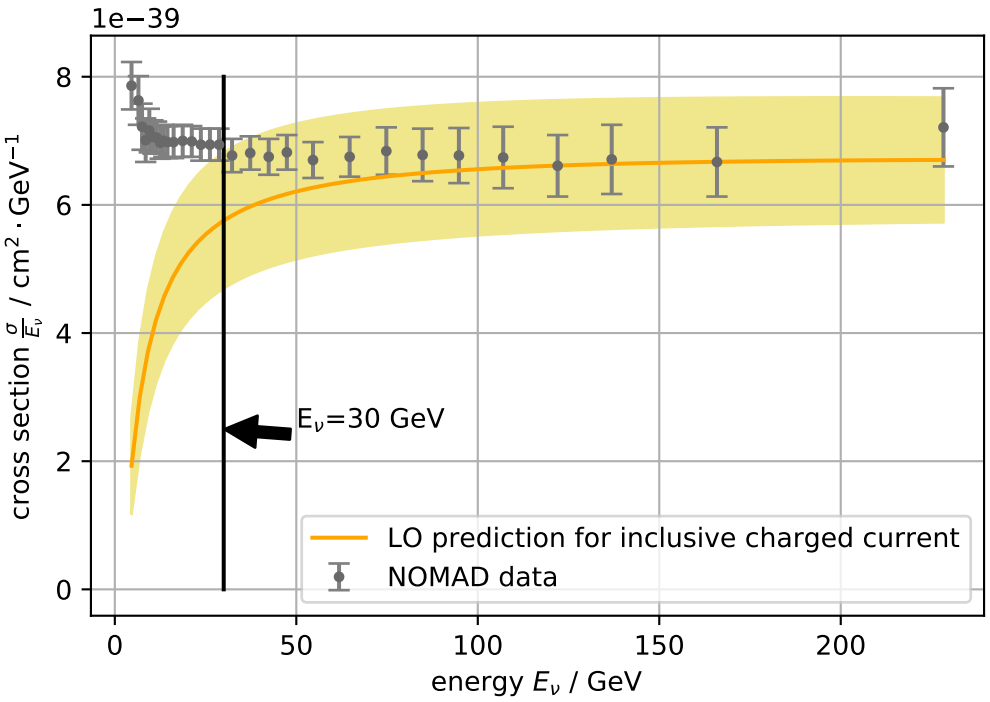


Figure 15: Inclusive charged current cross section in LO prediction compared with data from the NOMAD experiment

scattering and excited resonances [9]. Only above this energy does it enter the deep

inelastic scattering range. It can be seen that the deep inelastic scattering prediction describes the data well only from this energy and higher energies.
Finally, we look at the NOMAD ratio. The measured data were taken from [7]. They are shown in fig. 16 (grey). The blue plot represents the calculated ratio from eq. (65) with its

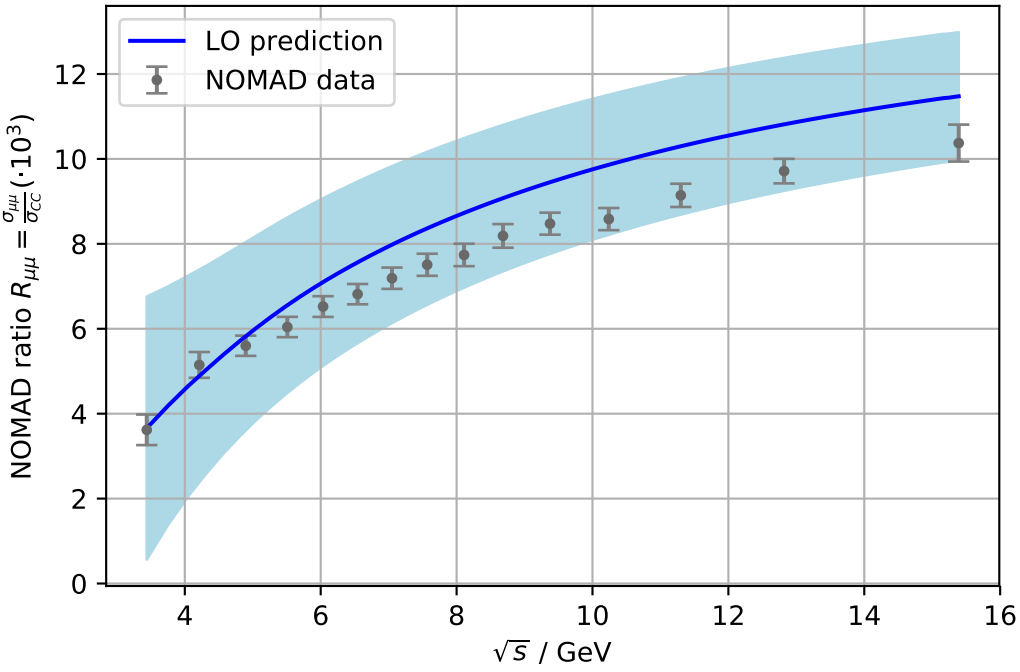


Figure 16: Comparison between the theoretical predictions for the NOMAD ratio in leading-order and the experimental data measured by the NOMAD experiment

uncertainty, calculated with the same PDF set. In fact, the data agree with the prediction of the calculation in its uncertainty range. It is important to note that according to the considerations from the previous plot, the values in the <30 GeV range should be viewed with caution. In this range of resonances, an error is made in the measurement in both the numerator and the denominator, which fortunately has a relatively equal effect, but cannot be quantised exactly. Calculations in next-to-leading-order and next-to-next-to-leading-order perturbation theory can describe the data even more precisely and with lower uncertainties [3]. In addition, the heavy quarks (charm, bottom and top) and the momentum component carried by the gluons were neglected in this calculation.

# 6 Conclusion and outlook

The first part of this thesis has shown that the idea of the proton as an elementary particle has been replaced by the knowledge that the proton consists of a complex inner structure of quarks and gluons. To describe this structure, the master formula of the

Parton model was derived in leading order perturbation theory. Then considerations have been made as to how the ratio of strange quarks in the proton can be determined by scattering experiments, because in contrast to the up and down quarks, little is known about the strange distribution. For this purpose, scattering with neutrinos was considered, since the weak interaction ensures the separation of individual strange distributions. In the last part the NOMAD ratio was reproduced with the NNPDF3 PDF sets in the leading order of perturbation theory.
The structure of the proton is still unexplored, but experiments like the NOMAD experiment are on their way to bring light into the darkness. The work with next-to-next-to-leading-order in perturbation theory provides a precise determination of the strangeness content of the proton. The results suggest that the proton is not too strange and carries only 65 to 80 per cent of the momentum fraction that the other light seaquarks carry. [3]. What will we be able to learn from the proton in the future? The precise knowledge about the strange quarks in the proton can be used to determine fundamental parameters of the Standard Model and it can be the baseline in the determination of nuclear PDFs [3].

# References


[1] Mauro Anselmino, Francisco Caruso, Elliot Leader, and José Soares Barbosa. How the callan-gross relation may survive in the presence of spin 1 diquarks. *Anais da Academia Brasileira de Ciencias*, 68:154–159, 01 1996.

[2] Sayipjamal Dulat, Tie-Jiun Hou, Jun Gao, Marco Guzzi, Joey Huston, Pavel Nadolsky, Jon Pumplin, Carl Schmidt, Daniel Stump, and C.-P. Yuan. New parton distribution functions from a global analysis of quantum chromodynamics. *Physical Review D*, 93(3), feb 2016.

[3] Ferran Faura, Shayan Iranipour, Emanuele R. Nocera, Juan Rojo, and Maria Ubiali. The strangest proton? *The European Physical Journal C*, 80(12), dec 2020.

[4] Alan D. Martin Francis Halzen. *QUARKS AND LEPTONS: An Introductory Course in Modem Particle Physics*. JOHN WILEY & SONS, 1 edition, 1984.

[5] Tie-Jiun Hou, Jun Gao, T. J. Hobbs, Keping Xie, Sayipjamal Dulat, Marco Guzzi, Joey Huston, Pavel Nadolsky, Jon Pumplin, Carl Schmidt, Ibrahim Sitiwaldi, Daniel Stump, and C.-P. Yuan. New CTEQ global analysis of quantum chromodynamics with high-precision data from the LHC. *Physical Review D*, 103(1), jan 2021.

[6] Hung-Liang Lai, Pavel Nadolsky, Jonathan Pumplin, Daniel Stump, Wu-Ki Tung, and Chien-Peng Yuan. The strange parton distribution of the nucleon: global analysis and applications. *Journal of High Energy Physics*, 2007(04):089–089, apr 2007.

[7] NOMAD Collaboration. A precision measurement of charm dimuon production in neutrino interactions from the nomad experiment, 2013.

[8] A. De Roeck and R.S. Thorne. Structure functions. *Progress in Particle and Nuclear Physics*, 66(4):727–781, oct 2011.

[9] Q. Wu, S.R. Mishra, A. Godley, R. Petti, S. Alekhin, P. Astier, D. Autiero, A. Baldisseri, M. Baldo-Ceolin, M. Banner, G. Bassompierre, K. Benslama, N. Besson, I. Bird, B. Blumenfeld, F. Bobisut, J. Bouchez, S. Boyd, A. Bueno, S. Bunyatov, L. Camilleri, A. Cardini, P.W. Cattaneo, V. Cavasinni, A. Cervera-Villanueva, R. Challis, A. Chukanov, G. Collazuol, G. Conforto, C. Conta, M. Contalbrigo, R. Cousins, H. Degaudenzi, T. Del Prete, A. De Santo, L. Di Lella, E. do Couto e Silva, J. Dumarchez, M. Ellis, G.J. Feldman, R. Ferrari, D. Ferrère, V. Flaminio, M. Fraternali, J.-M. Gaillard, E. Gangler, A. Geiser, D. Geppert, D. Gibin, S. Gninenko, J.-J. Gomez-Cadenas, J. Gosset, C. Gößling, M. Gouanère, A. Grant, G. Graziani, A. Guglielmi, C. Hagner, J. Hernando, P. Hurst, N. Hyett, E. Iacopini, C. Joseph, F. Juget, N. Kent, J.J. Kim, M. Kirsanov, O. Klimov, J. Kokkonen, A. Kovzelev, A. Krasnoperov, S. Kulagin, S. Lacaprara, C. Lachaud, B. Lakić, A. Lanza, L. La Rotonda, M. Laveder, A. Letessier-Selvon, J.-M. Levy, J. Ling, L. Linssen, A. Ljubič, J. Long, A. Lupi, V. Lyubushkin, A. Marchionni, F. Martelli, X. Méchain, J.-P.

Mendiburu, J.-P. Meyer, M. Mezzetto, G.F. Moorhead, D. Naumov, P. Nédélec, Yu. Nefedov, C. Nguyen-Mau, D. Orestano, F. Pastore, L.S. Peak, E. Pennacchio, H. Pessard, A. Placci, G. Polesello, D. Pollmann, A. Polyarush, C. Poulsen, B. Popov, L. Rebuffi, J. Rico, P. Riemann, C. Roda, A. Rubbia, F. Salvatore, O. Samoylov, K. Schahmaneche, B. Schmidt, T. Schmidt, A. Sconza, M. Seaton, M. Sevior, D. Sillou, F.J.P. Soler, G. Sozzi, D. Steele, U. Stiegler, M. Stipčević, Th. Stolarczyk, M. Tareb-Reyes, G.N. Taylor, V. Tereshchenko, A. Toropin, A.-M. Touchard, S.N. Tovey, M.-T. Tran, E. Tsesmelis, J. Ulrichs, L. Vacavant, M. Valdata-Nappi, V. Valuev, F. Vannucci, K.E. Varvell, M. Veltri, V. Vercesi, G. Vidal-Sitjes, J.-M. Vieira, T. Vinogradova, F.V. Weber, T. Weisse, F.F. Wilson, L.J. Winton, B.D. Yabsley, H. Zaccone, K. Zuber, and P. Zuccon. A precise measurement of the muon neutrino – nucleon inclusive charged current cross section off an isoscalar target in the energy range 2.5<$E_\nu$<30 GeV by NOMAD. *Physics Letters B*, 660(1-2):19–25, feb 2008.

# A Appendix

In the following section, the relations and theoretical background from [4] required for the calculation of the cross sections are presented.

## A.1 Dirac equation

The Dirac equation is a relativistically generalised form of the Schrödinger equation. It reads:

$$H\psi = (\vec{\alpha}\vec{P} + \beta m)\psi$$

This equation must satisfy the relativistic energy-momentum relation, i.e.

$$H^2\psi = (P^2 + m^2)\psi$$

It can be seen that all $\alpha_i$ and $\beta$ must anticommute with each other and furthermore $\alpha_1^2 = \alpha_2^2 = \alpha_3^2 = \beta^2 = 1$ must be given. Since the coefficients do not commute with each other, they cannot be scalar prefactors, but have the form of 4x4 matrices. These are the so-called Dirac-Pauli matrices. The conventionally used representation of the matrices is

$$\vec{\alpha} = \begin{pmatrix} 0 & \vec{\sigma} \\ \vec{\sigma} & 0 \end{pmatrix} \quad \beta = \begin{pmatrix} \mathbb{1}_{2\times2} & 0 \\ 0 & -\mathbb{1}_{2\times2} \end{pmatrix}. \tag{A.1}$$

It is called the Dirac Pauli representation. The $\sigma$ matrices are the Pauli matrices:

$$\sigma_1 = \begin{pmatrix} 0 & 1 \\ 1 & 0 \end{pmatrix} \quad \sigma_2 = \begin{pmatrix} 0 & -i \\ i & 0 \end{pmatrix} \quad \sigma_1 = \begin{pmatrix} 1 & 0 \\ 0 & -1 \end{pmatrix}$$

A four-vector that satisfies the Dirac equation is called a Dirac spinor.
It is useful to consider the Dirac equation in covariant form:

$$(i\gamma^\mu\partial_\mu - m)\psi = 0 \tag{A.2}$$

Here $\gamma^\mu = (\beta, \beta\vec{\alpha})$. If one additionally introduces the adjoint line vector $\overline{\psi} = \psi^\dagger\gamma^0$ one can derive from the hermitian conjugate Dirac equation

$$i\partial_\mu\overline{\psi}\gamma^\mu + m\overline{\psi} = 0.$$

From the two equations the continuity equation $\partial_\mu j^\mu = 0$ can be derived and it results in

$$j^\mu = \overline{\psi}\gamma^\mu\psi.$$

The probability density $\rho = j^0 = \overline{\psi}\gamma^0\psi = \psi^\dagger\psi = \sum_{i=1}^4 |\psi_i|^2 \geq 0$ is positively defined, unlike the solution in the Klein-Gordan equation, which was Dirac's original aim.

For a free particle, the eigensolutions of the Dirac equation are $\psi = u(p)e^{ipx}$. $u$ is a four-component spinor that is independent of $x$. The Dirac equation simplifies to

$$\begin{aligned} Hu &= (\vec{\alpha} + \beta m)u = Eu \\ &= \begin{pmatrix} m & \vec{\sigma}\vec{p} \\ \vec{\sigma}\vec{p} & -m \end{pmatrix} \begin{pmatrix} u_A \\ u_B \end{pmatrix} = E \begin{pmatrix} u_A \\ u_B \end{pmatrix}. \end{aligned} \tag{A.3}$$

The solutions of the equation are

$$\begin{aligned} u^{(s)} &= N \begin{pmatrix} \chi^{(s)} \\ \frac{\vec{\sigma}\cdot\vec{p}}{E+m}\chi^{(s)} \end{pmatrix}, \qquad E > 0, \quad s = 1, 2 \\ u^{(s+2)} &= N \begin{pmatrix} -\frac{\vec{\sigma}\cdot\vec{p}}{|E|+m}\chi^{(s)} \\ \chi^{(s)} \end{pmatrix}, \qquad E < 0. \end{aligned}$$

It should be noted that all 4 solutions are orthogonal to each other. The Dirac equation yields an additional twofold degeneracy. In order to cancel this degeneracy, an additional observable is sought which commutes with $\hat{P}$ as well as with $\hat{H}$. For this, the spin component in the direction of motion $\frac{1}{2}\vec{\sigma}\cdot\vec{p}$ (for spin $\frac{1}{2}$ particles) is chosen, the so-called helicity.

## A.2 Dirac-gamma matrices and trace theorems

In the Dirac-Pauli representation, the $\gamma$ matrices have the form

$$\gamma^0 = \begin{pmatrix} \mathbb{1}_{2\times2} & 0 \\ 0 & -\mathbb{1}_{2\times2} \end{pmatrix} \qquad \beta = \begin{pmatrix} 0 & \vec{\sigma} \\ -\vec{\sigma} & 0 \end{pmatrix}.$$

By recalculation the following identities result ($k = 1, 2, 3$):

$$\left.\begin{aligned} \gamma^{k\dagger} &= \gamma^0\gamma^k\gamma^0 \\ \gamma^{k\dagger} &= -\gamma^k \end{aligned}\right\} \{\gamma^0, \gamma^k\} = 0 \quad \text{(anticommutator)}$$

$$\begin{aligned} \gamma^{0\dagger} &= \gamma^0 \qquad \gamma^{0\,2} = \mathbb{1}_{4\times4} \\ \gamma^\mu\gamma^\nu + \gamma^\nu\gamma^\mu &= 2g^{\mu\nu} \end{aligned} \tag{A.4}$$

To be able to represent particle currents in their most general form, it is useful to introduce $\gamma^5 = i\gamma^0\gamma^1\gamma^2\gamma^3$. In the Dirac-Pauli representation $\gamma^5$ has the form

$$\gamma^5 = \begin{pmatrix} 0 & \mathbb{1}_{2\times2} \\ \mathbb{1}_{2\times2} & 0 \end{pmatrix}$$

For $\gamma^5$ it applies

$$\begin{aligned} \gamma^{5\dagger} &= \gamma^5 \\ \gamma^{5\,2} &= \mathbb{1}_{4\times4} \\ \{\gamma^5, \gamma^\mu\} &= 0 \quad \text{(anticommutator)}. \end{aligned}$$

For the traces of different combinations of the $\gamma$-matrices, the following trace theorems apply:

$$\begin{aligned}
\mathrm{Tr}(\gamma^\mu\gamma^\nu) &= 4g^{\mu\nu} \\
\mathrm{Tr}(\gamma^\mu\gamma^\nu\gamma^\rho\gamma^\sigma) &= 4(g^{\mu\nu}g^{\rho\sigma} - g^{\mu\rho}g^{\nu\sigma} + g^{\mu\sigma}g^{\nu\rho}) \\
\mathrm{Tr}(\gamma^5\gamma^\mu\gamma^\nu) &= 0 \\
\mathrm{Tr}(\gamma^5\gamma^\mu\gamma^\nu\gamma^\rho\gamma^\sigma) &= 4i\epsilon^{\mu\nu\rho\sigma}
\end{aligned}$$

The trace for an odd number of $\gamma$ matrices multiplied together is always 0.

## A.3 Feynman rules

- External lines
  - Spin 0 boson: 1
  - Spin $\frac{1}{2}$fermion (in,out): $u$, $\bar{u}$
  - Spin $\frac{1}{2}$ antifermion: $v$,$\bar{v}$
  - Spin 1 photon: $\epsilon_\mu$,$\epsilon^*_\mu$
- Internal lines
  - Spin 0 boson: $\frac{i}{p^2-m^2}$
  - Spin $\frac{1}{2}$ fermions: $\frac{i(\not{p}+m)}{p^2-m^2}$
  - Spin 1 photon: $\frac{-ig_{\mu\nu}}{p^2}$
- Vertex factor
  - photon - spin $\frac{1}{2}$ fermion: $ie\gamma^\mu$
  - boson - spin $\frac{1}{2}$ fermion: $ie\frac{1}{2}\gamma^\mu(1-\gamma^5)$

## A.4 Mandelstam variables

For the process $AB \to CD$ one defines the Lorentz invariant variables:

$$\begin{aligned}
s &= (p_A + p_B)^2 = (p_C + p_D)^2 = m_A^2 + 2p_Ap_B + m_B^2 = m_C^2 + 2p_Cp_D + m_D^2 \\
t &= (p_A - p_C)^2 = (p_B - p_D)^2 = m_A^2 - 2p_Ap_C + m_C^2 = m_B^2 - 2p_Bp_D + m_D^2 \\
u &= (p_A - p_D)^2 = (p_B - p_C)^2 = m_A^2 - 2p_Ap_D + m_D^2 = m_B^2 - 2p_Bp_C + m_C^2
\end{aligned}$$

In the extreme-relativity limit, all masses can be neglected and it holds:

$$\begin{aligned}
s &= 2p_Ap_B = 2p_Cp_D \\
t &= -2p_Ap_C = -2p_Bp_D \\
u &= -2p_Ap_D = -2p_Bp_C
\end{aligned} \tag{A.5}$$

In the CMS, the impulses of the incoming particles as well as those of the outgoing particles must be equal in terms of magnitude and thus (with negligible masses) also the energies. Since conservation of energy also applies, all energies must be equal after and before the collision. The following applies

$$\begin{aligned} \vec{p_A} = -\vec{p_B} \quad \vec{p_C} = -\vec{p_D} \\ |\vec{p_A}| = |\vec{p_B}| = E = |\vec{p_C}| = |\vec{p_D}| \end{aligned}$$

In this case, the following applies to the Mandelstam variables:

$$\begin{aligned} s &= 4E^2 \\ t &= -2E^2(1-\cos\theta) = -\frac{1}{2}s(1-\cos\theta) \\ u &= -2E^2(1+\cos\theta) = -\frac{1}{2}s(1+cos\theta) \end{aligned} \tag{A.6}$$

Here $\theta$ denotes the scattering angle between A and C.
If the mass $M$ of particle B is not negligible, it makes sense to consider the scattering process in the laboratory system, i.e. the system in which particle B is at rest. The four momentum of particle B is then $p_B = (M, 0)$. $E$ and $E'$ denote the energies of the other particle before (A) and after (C) the scattering. In this case, the Mandelstam variables can be expressed as

$$\begin{aligned} s &= 2ME \\ t &= -2EE'(1-\cos\theta) \\ u &= -2ME' \end{aligned} \tag{A.7}$$

## A.5 Substitution of invariant variables

For a t-channel process we have

$$Q^2 = -t = 2EE'(1-\cos\theta) = 4EE'\sin^2\frac{\theta}{2} \tag{A.8}$$

$$v = \frac{p\cdot q}{p\cdot k} \underbrace{=}_{\text{CMS}} = E - E' \tag{A.9}$$

It is easy to see that $Q^2$ and $v$ are lorentz invariant, because the scalar product of two four-vectors is always Lorentz invariant. Therefore, $v$ can be considered in the CMS without changing anything. We can also consider the differential cross sections according to these variables instead of according to $d\Omega dE'$. This results in:

$$\begin{aligned} d\Omega = 2\pi d\cos\theta = -\frac{\pi}{EE'}dQ \\ dE' = -dv \\ dE'd\Omega = \frac{\pi}{EE'}dQ^2dv \end{aligned} \tag{A.10}$$

We define

$$\begin{aligned} y &= \frac{p\cdot q}{p\cdot k} \underbrace{=}_{\text{CMS}} \frac{E-E'}{E} = \frac{v}{E} \\ x &= \frac{Q^2}{2p\cdot q} = \frac{Q^2}{2Mv} = \frac{Q^2}{2MEy} \\ x\cdot y &= \frac{Q^2}{2ME} \end{aligned} \tag{A.11}$$

Also, $x$ and $y$ are Lorentz invariant, which can be recognised by the fact that they are only defined via scalars and scalar products of four-vectors. This results in:

$$\begin{aligned} dv &= Edy \\ dQ^2 &= 2MEydx \\ dQ^2dv &= 2E^2My\ dxdy \end{aligned} \tag{A.12}$$

With the definitions of $s$, $t$ and $u$ from the previous section, the following relations can be recorded:

$$\begin{aligned} x &= -\frac{t}{s+u} \\ y &= \frac{Q^2}{2ME}\frac{1}{x} = \frac{t}{s}\frac{s+u}{t} = 1+\frac{u}{s} \\ dy &= \frac{1}{s}du \\ dx &= -\frac{1}{s+u}ds \\ dxdy &= -\frac{1}{s(s+u)}dtdu \end{aligned} \tag{A.13}$$

## A.6 Initial flux

The initial flux is defined as

$$F = 4|v_k - v_P|E_kE_P = 4(|\vec{k}|E_P + |\vec{P}|E_k). \tag{A.14}$$

with

$$\begin{aligned} (P\cdot k)^2 &= (E_kE_P - |\vec{k}||\vec{P}|)^2 = (E_k^2E_P^2 - 2E_kE_P|\vec{k}||\vec{P})| + |\vec{k}|^2|\vec{P}|^2) \\ m_P^2m_k^2 &= (E_P^2 - |\vec{P}|^2)(E_K^2 - |\vec{k}|^2) = E_k^2E_P^2 - E_P^2|\vec{k}|^2 - E_k^2|\vec{P}|^2 + |\vec{P}|^2|\vec{k}|^2 \end{aligned}$$

$$\Rightarrow (|\vec{k}|E_P + |\vec{P}|E_k) = \sqrt{(P\cdot k)^2 - m_P^2m_k^2}$$

So the initial flux can be expressed as

$$F = 4\sqrt{(P\cdot k)^2 - m_P^2m_k^2} \tag{A.15}$$

which is Lorentz-invariant in any case. In the case of a negligible mass $m_K$ and the observation from the laboratory system, i.e. the mass $m_p$ at rest , the following results

$$F = 4ME_k \tag{A.16}$$

## A.7 lorentz-invariant phase space factor

Starting from the definition of the phase space factor, this is expressed in the following in different ways

$$\begin{aligned} dQ_1 &= \frac{d^3\vec{k'}}{2E'(2\pi)^3} && \text{Change to spherical coordinates} \\ &= \frac{|k'|^2 d|k'| d\Omega}{2E'(2\pi)^3} && m \approx 0 \rightarrow |k'|^2 d|k'| = E'^2 dE' \\ &= \frac{E' dE' d\Omega}{2(2\pi)^3} \end{aligned} \tag{A.17}$$

$$dQ_2 = \frac{d^3\vec{k'}}{(2\pi)^3 2E_{k'}} \frac{d^3\vec{P'}}{(2\pi)^3 2E_{P'}} (2\pi)^4 \delta^{(4)}(k + P - k' - P')$$

$$= \frac{d^3\vec{k'}}{(2\pi)^3 2E_{k'}} \frac{d^4P'}{(2\pi)^3} \delta(P'^2 - m_P'^2)(2\pi)^4 \delta^{(4)}(k + P - k' - P') \qquad \text{|Integrate } d^4P'$$

$$= \frac{d^3\vec{k'}}{(2\pi)^3 2E_{k'}} (2\pi)\delta((k + P - k')^2 - m_p^2) \qquad \text{|Change to spherical coordinates}$$

$$= \frac{|k'|^2 d|k'| d\Omega}{8\pi^2 E_{k'}} \delta((k + P - k')^2 - m_p^2) \qquad |q = k - k', \text{ und } |k'|d|k'| = E_{k'} dE_{k'}$$

$$= \frac{E' dE_{k'} d\Omega}{8\pi^2} \delta((P + q)^2 - m_p^2)$$

$$= \frac{E' dE_{k'} d\Omega}{8\pi^2} \delta(2p \cdot q + q^2) \qquad \text{|Switch to the lab. frame: fruther on } dQ_{\text{Lab}}$$

$$= \frac{E' dE_{k'} d\Omega}{8\pi^2} \delta(2Mv + q^2)$$

$$= \frac{E' dE_{k'} d\Omega}{16\pi^2 M} \delta(v + \frac{q^2}{2M}) \tag{A.18}$$

$$dQ_{\text{Lab}} = \frac{E' dE_{k'} d\Omega}{8\pi^2} \delta(2M_P(E - E') - 4EE' \sin^2 \frac{\Theta}{2}))$$

$$= E' dE_{k'} d\Omega \frac{1}{8\pi^2 2M_P} \delta(E - E' - \frac{2EE'}{M_P} \sin^2 \frac{\Theta}{2})) \qquad \text{with } A = 1 + \tfrac{2E}{M_P} \sin^2 \tfrac{\Theta}{2}$$

$$= E' dE_{k'} d\Omega \frac{1}{16\pi^2 m_P A} \delta(E' - \frac{E}{A}) \tag{A.19}$$

$$dQ_{\text{CMS}} = \frac{1}{(2\pi)^3 2E_{k'}} \frac{d^3\vec{P'}}{(2\pi)^3 2E_{P'}} (2\pi)^4 \delta(E_k + E_p - E_{k'} - E_{p'}) \qquad \text{mit } E_k + E_p = \sqrt{s} = W$$

$$= \frac{1}{(2\pi)^2 2E_{k'}} \frac{d^3\vec{p'}}{2E_{P'}} \delta(W - E_{k'} - E_{p'}) \qquad \text{Change to spherical coordinates}$$

$$= \frac{1}{4\pi^2} \frac{|\vec{p'}|^2 d|p'| d\Omega}{4E_{k'} E_{p'}} \delta(W - E_{k'} - E_{p'}) \tag{A.20}$$

At this point it can be exploited that

$$W = E_{k'} + E_{p'} = \sqrt{(m_k^2 + p_f^2)} + \sqrt{(m_p^2 + p_f^2)}$$

Here $p_f = |\vec{k'}| = |\vec{p'}|$ is the momentum of the particles after the scattering, which has the same magnitude in the CMS for both particles. We now use the relation

$$\frac{dW}{dp_f} = p_f(\frac{1}{E_{k'}} + \frac{1}{E_{p'}}) = p_f \frac{E_{k'} + E_{p'}}{E_{k'} E_{p'}}$$

to replace $dp_f$ with $dW$. Insertion yields:

$$\begin{aligned} dQ_{\mathrm{CMS}} &= \frac{1}{4\pi^2}\frac{p_f dW d\Omega}{4(E_{k'}+E_{p'})}\delta(W-E_{k'}-E_{p'}) \\ &= \frac{1}{4\pi^2}\frac{p_f}{4\sqrt{s}}d\Omega \end{aligned} \tag{A.21}$$

## A.8 Product of the 4-dimensional Epsilon-Tensor

$$\begin{aligned} \epsilon^{\mu\alpha\nu\beta}\epsilon_{\mu\kappa\nu\lambda} &= -2\delta^{\alpha\beta}_{\kappa\lambda} \\ &= -2[\delta^{\alpha}_{\kappa}\delta^{\beta}_{\lambda} - \delta^{\alpha}_{\lambda}\delta^{\beta}_{\kappa}] \end{aligned} \tag{A.22}$$

## Eigenständigkeitserklärung

Hiermit versichere ich, dass die vorliegende Arbeit über Dimuon production in deep inelastic scattering selbstständig von mir und ohne fremde Hilfe verfasst worden ist, dass keine anderen Quellen und Hilfsmittel als die angegebenen benutzt worden sind und dass die Stellen der Arbeit, die anderen Werken – auch elektronischen Medien – dem Wortlaut oder Sinn nach entnommen wurden, auf jeden Fall unter Angabe der Quelle als Entlehnung kenntlich gemacht worden sind. Mir ist bekannt, dass es sich bei einem Plagiat um eine Täuschung handelt, die gemäß der Prüfungsordnung sanktioniert werden kann.

Ich erkläre mich mit einem Abgleich der Arbeit mit anderen Texten zwecks Auffindung von Übereinstimmungen sowie mit einer zu diesem Zweck vorzunehmenden Speicherung der Arbeit in einer Datenbank einverstanden.

Ich versichere, dass ich die vorliegende Arbeit oder Teile daraus nicht anderweitig als Prüfungsarbeit eingereicht habe.

15.08.2022, U. Gruel
(Datum, Unterschrift)